Palynology of the Recent Intertidal Sediments of the Southern Red Sea Coast of Saudi Arabia

Author: Kumar, Arun

Source: Palynology, 45(1) : 143-163

Published By: AASP: The Palynological Society

URL: https://doi.org/10.1080/01916122.2020.1767708

PALYNOLOGY
2021, VOL. 45, NO. 1, 143–163
https://doi.org/10.1080/01916122.2020.1767708

Palynology of the recent intertidal sediments of the Southern Red Sea Coast of Saudi Arabia

Arun Kumar

Department of Earth Sciences, Carleton University, Ottawa, ON, Canada

ABSTRACT

Seven semi-consolidated surface sediment samples from the tidal flats along the southern Red Sea coast of Saudi Arabia were studied for their palynomorph assemblages. These samples are mainly clay and fine sand and yielded low numbers but high diversity of palynomorphs. They have various affinities and have been divided into five groups: (A) pollen and spores; (B) dinoflagellate cysts and algal remains; (C) fungal spores, hyphae and fruit bodies; (D) protists and invertebrate remains; and (E) miscellaneous and unidentified forms. The protists and invertebrate remains are a diverse group that includes microforaminifera, thecamoebians, tintinnomorphs, crustacean and annelid palynomorphs. These palynomorphs belong to both marine and terrestrial environments and are of autochthonous and allochthonous origins. An attempt has been made to identify each palynomorph and relate it to its parent organism, plant or animal, and to discuss its environment. This is the first such study in and around the Arabian Peninsula.

KEYWORDS

Red Sea Recent sediments; intertidal environments; non-pollen palynomorphs (NPP); palynology; micropalaeontology; Saudi Arabia

Introduction

During the past few decades, non-pollen palynomorphs (NPP), including their identification and source, have become an important part of palynological studies. Most NPP found in the palynological preparations of past studies were ignored, and emphasis was primarily concentrated on pollen, spores, dinoflagellate cysts and, to a lesser extent, fungal remains. Such NPP studies were initiated in Europe with the examination of a variety of sediments from different freshwater depositional environments (van Geel 1972, 1976, 1986, 2001). Other studies from freshwater environments have been made in Africa (Gelorini et al. 2012), Australia (Cook 2009), Canada (Warner 1990; McCarthy et al. 2011, 2018), India (Limaye et al. 2007, 2017), Venezuela (Montoya et al. 2010) and several more locations. NPP studies from marine and marginal marine environments were initiated later; examples include Canada (de Vernal 2009), Costa Rica (Medeanic et al. 2008), England (Head 1993), Indonesia (van Waveren 1992, 1994), Malaysia and Oman (Matsuoka et al. 2017), and the Mediterranean region (Kholeif 2007; Kholeif and Mudie 2009). The earliest micropalaeontological studies on environmental changes in the Red Sea in the Late Pleistocene–Holocene (past 80,000 years) used micropalaeontologic data (on dinoflagellates, foraminifera, nannofossils, pteropods and radiolarians) along with radiocarbon dates (Berggren 1969; Wall and Warren 1969). These studies have strengthened palynological research in defining diverse aspects of palaeoenvironmental and palaeoecological interpretations.

Most papers pertinent to the present research are from NPP studies in the Black Sea corridor (Mudie et al. 2010) and the Caspian–Black Sea–Mediterranean corridor (Mudie et al. 2011). No such study has ever been published from the Arabian Peninsula, except for a preliminary report on two offshore Oman samples by Matsuoka et al. (2017). Similar studies were published from Egypt by Kholeif (2004, 2007). Recent dinoflagellate cysts were described from the Persian Gulf, Gulf of Oman and northwestern Arabian Sea (Bradford 1975; Bradford and Wall 1984). However, no such study has ever been published on the Red Sea coastal sediments. The objectives of the present study were to identify all palynomorphs including NPP from the intertidal sediments of the southern Red Sea coast of Saudi Arabia and to determine their sources and environments. Palynomorphs in the intertidal sediments are autochthonous and allochthonous and were sourced from marine and terrestrial environments. NPP are mostly microscopic parts belonging to a variety of plants, algae, fungi, protists and invertebrates, or to a lesser extent whole organisms such as dinoflagellate cysts.

The Red Sea

The Red Sea is a long and narrow body of water separating northeast Africa to the west from the Arabian Peninsula to the east (Figure 1). It joins the Gulf of Aden at its southern end through the Bab el Mandeb Strait, and its northern end is bifurcated into two narrow, elongated water bodies on either side of the Sinai Peninsula. On the west side is the Gulf of Suez and on the east side is the Gulf of Aqaba.

CONTACT Arun Kumar arunkumarlko@hotmail.com Department of Earth Sciences, Carleton University, Ottawa, ON K1S 5B6, Canada.

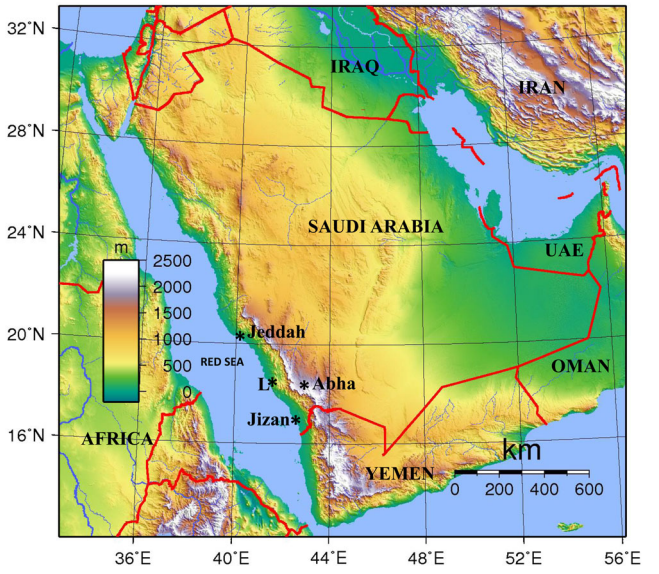

Figure 1. Topographical map of the Arabian Peninsula showing locations of various countries and the Red Sea. Study location is marked with an 'L' (modified after https://commons.wikimedia.org/wiki/File:Saudi_Arabia_Topography.png).

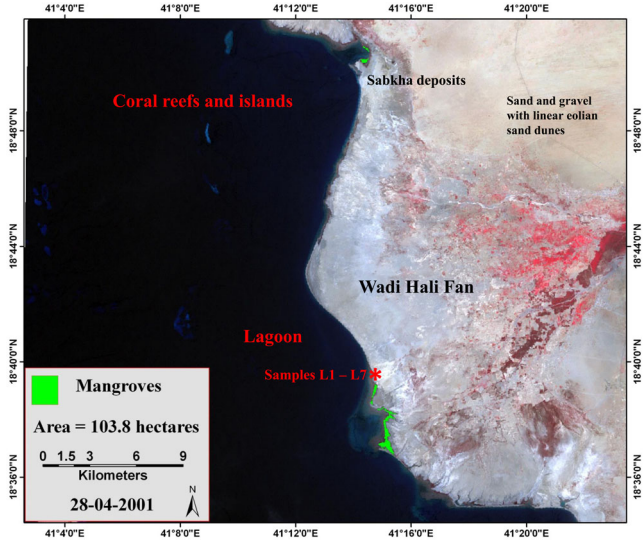

Figure 2. Coastal and terrestrial environments around the area of study. Satellite image of the area showing marine and coastal environments. Mangroves shown in green (modified after Khan et al. 2010).

Surface water temperatures are constant year-round at 21–25 °C (Jado and Zölt 1984). Its salinity ranges between ~36‰ (3.6% on the Practical Salinity Scale or PSU, meaning actual dissolved salts) in the southern region and ~ 41‰ (4.0% PSU) in the northern region, whereas the world average is ~35‰ or 3.5% PSU (Hanauer 1988).

Since it is a semi-enclosed basin located within an arid region, it is affected by high rates of evaporation, high temperatures and high salinities. These conditions in the Red Sea govern the composition of the flora and fauna of the sea and along its coast. Extensive coral reefs fringe the sea. The coastal areas are undergoing rapid urbanisation that is causing stress on the environment in many areas (Rasul and Stewart 2015).

The climate of the Red Sea is the result of two distinct monsoon seasons: a northeasterly monsoon and a southwesterly monsoon. The rainfall over the Red Sea coast is extremely low, averaging 0.06 m/year; this is mostly in the form of showers of short duration, often associated with thunderstorms and occasionally with dust storms. During the summer, northwest winds drive surface water south, whereas in winter the flow is reversed, resulting in the inflow of water from the Gulf of Aden into the Red Sea. The net value of the latter predominates, resulting in an overall drift to the northern end of the Red Sea. Thus, the prevailing north and northeastern winds influence the movement of water in the coastal inlets to the adjacent sabkhas (saltpans), especially during storms. The winter mean sea level is 0.5 m higher than the mean sea level in the summer (Kumar et al. 2010).

This long Red Sea coastline covers both tropical and subtropical zones. Surface water temperatures increase southward in response to latitude, but the salinity of the surface water increases northwards. Intrusion of low-salinity water from the Gulf of Aden into the Red Sea causes lower water salinity in the southern Red Sea. The tidal amplitude along the Red Sea coast is only ~50 cm on the northern and southern coasts, and it gradually decreases towards the centre, reaching close to zero near Jeddah (Khan et al. 2010; Kumar et al. 2011).

Coastal sediments of the Wadi Hali quadrangle

The Red Sea coast of Saudi Arabia is an arid region covered by Quaternary terraced alluvial deposits, eolian sands, riverbed alluvium and sabkhas; the region is known as the Tihama (also spelled Tihamah) Plain. Mangrove swamps and wadis (dry riverbeds) are scattered along the coast. The area of the present study falls within the Wadi Hali (also spelled Haliy) Fan that lies on the Red Sea coast of Saudi Arabia, south of Jeddah and north of Jizan (Figures 2, 3). This is a small region covering an area around 50 km N-S and 40 km E-W. This area has several distinct depositional environments, including aeolian, fluvial, coastal, intertidal, brackish-water ponds with mangrove stands, and saline lagoons. Estuarine clastic sediments have been deposited in this region since Miocene. The process of erosion and deposition of wadis and eolian sediments has been going on since the beginning of the Quaternary (Jado et al. 1990).

Due to Quaternary sea-level changes, diverse types of coastal environments developed, ranging from open shelf basins to fringing, barrier or patch reefs and various littoral environments (Jado and Zölt 1984; Jado et al. 1990). Many coral reef islands of various sizes and shapes are present; some are near the shore and others are far offshore in the Red Sea (Figure 2). Several lagoons and bays, both small and large, meander through this long coastline, and at times become saline lakes because they get disconnected from the sea due to either local tectonics or Quaternary sea-level changes. Many fluvial channels originate in the mountains towards the east that carry water and sediments into the Red Sea (Khan et al. 2010).

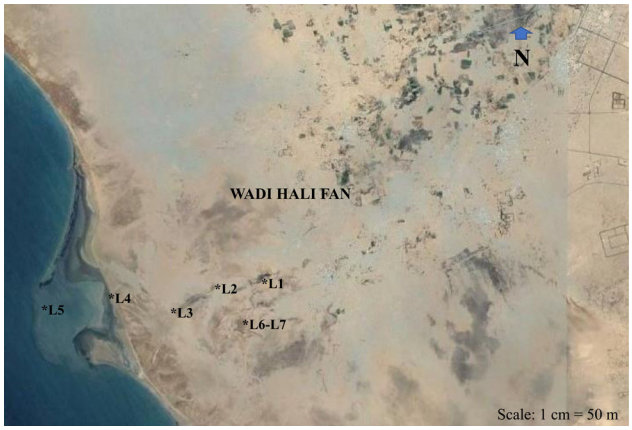

Figure 3. A close-up of the area where samples (L1 through L7) were collected, showing the sample localities.

Coastal flora and vegetation

A study on the vegetation types of the Red Sea coast south of Jedda by Vesey-Fitzgerald (1955) was the pioneering work in Saudi Arabia. The two-volume publication on the *Flora of Saudi Arabia* by Migahid (1978) is an important reference on the subject. The website 'Plant Diversity in Saudi Arabia' is also a significant source of information about the vegetation and flora of Saudi Arabia (Thomas 2011). This website was created and is presently managed by Dr Jacob Thomas, Department of Botany and Microbiology, King Saud University, Riyadh, Saudi Arabia. It provides valuable information about vegetation types and their floral elements in southwestern Saudi Arabia, including the Red Sea coast. According to this website there are five broad categories of vegetation in Saudi Arabia: (1) vegetation of the coastal plains and sabkhas; (2) deserts and scarcely vegetated areas; (3) dwarf shrub-lands; (4) woodlands and xeromorphic shrub-lands of high-altitude areas; and (5) wadi communities. The coastal zone where the present study was carried out is characterised by low sand dunes and saline marshes, and the vegetation is generally scattered and poor in such terrains (Figure 4). This zone is characterised by open, drought-deciduous thorn woodlands, and has mangroves, halophytes, open xeromorphic grasslands and thorn woodlands (Figure 4).

The distribution of mangroves is patchy; they are generally restricted to the quieter, low-energy environments such as bays, narrow channels, and inland faces of offshore islands. However, they also occur in the intertidal environments. Along the Red Sea coast, *Avicennia marina* is the dominant species, but *Rhizophora mucronata* occurs in patches on the Farasan Islands (Khan et al. 2010) as well.

Study area

The study site is located west of the town of Abha on the southern Red Sea coast of Saudi Arabia, between Jeddah to the north and Jizan to the south (Figure 1). This area covers Wadi Hali and its surroundings (180°49′35.27″N, 410°22′44.23″E). Wadi Hali is a short ephemeral stream that originates in the hilly regions east of the coastal region (Figures 1 and 2).

The area under the present study covers mainly a mixture of marginal marine and non-marine environments that include upper intertidal and supratidal flats. Microbial mats and mud flats; scattered patches of mangrove stand and their muddy environments; and sand flats, both rippled and without ripples of the upper intertidal environments, are covered in this study (Figures 3 and 5).

Quaternary climate

There have been numerous studies dealing with Quaternary climate fluctuations and their influence on the formation of vast deserts, sand dunes and sabkhas in the Arabian Peninsula. Climatic variability between periods of relative aridity and humidity during the Quaternary has led to the development of various sedimentary environments such as alluvial fans, inland and coastal sand dunes and sabkhas.

Studies on the palaeo-lake deposits from the Rub al Khali desert of the southern Arabian Peninsula indicate that pluvial conditions (wetter than today) were related to interglacial periods. Such pluvial periods in the southern regions of the Arabian Peninsula existed from 33–24 ka BP and 9–5 ka BP, and such milder climate regimes supported savanna to open deserts (Grainger 2007). During glacial periods in the high latitudes, global sea levels were low, and quartz sands from the exposed bottom of the Arabian Gulf were thereby transported by Shamal winds southeastward to the UAE and then on to the Rub al Khali; however, during the interglacial period this supply of sand from the bottom of the Arabian Gulf was cut off due to high sea-level stands. There are two main wind systems in the region: first, the Shamal, a winter wind that blows southwards over the Arabian Gulf towards UAE, then turns clockwise across the Rub al Khali; and second, the southwest monsoon, a summer wind that blows across the Arabian Sea from northeast Africa to India, with a branch that veers north towards the Arabian Peninsula.

An overview of the natural hazards of the Arabian Peninsula by the author (Kumar 2013) mentioned that among other natural hazards, sand and dust storms and flash floods occur frequently and cause serious damage to the health and property of humans in the region. Flash floods are caused by heavy rainfall from a stationary front, hurricane, tropical storm or thunderstorms. The average annual rainfall in coastal Arabia is <5 cm; thus, the fluvial influx is very low and is limited to occasional flooding of desert wadis due to rains. These natural processes influence the transport of microscopic biological entities from one place to another.

Materials and methods

For this study, seven samples (L1 through L7) were collected during a geological field trip to the southern Red Sea coast of Saudi Arabia in the first week of March 2011. They are surface semi-consolidated sediments from the tidal flats, a small pond on the tidal flats and the subtidal environment. Four

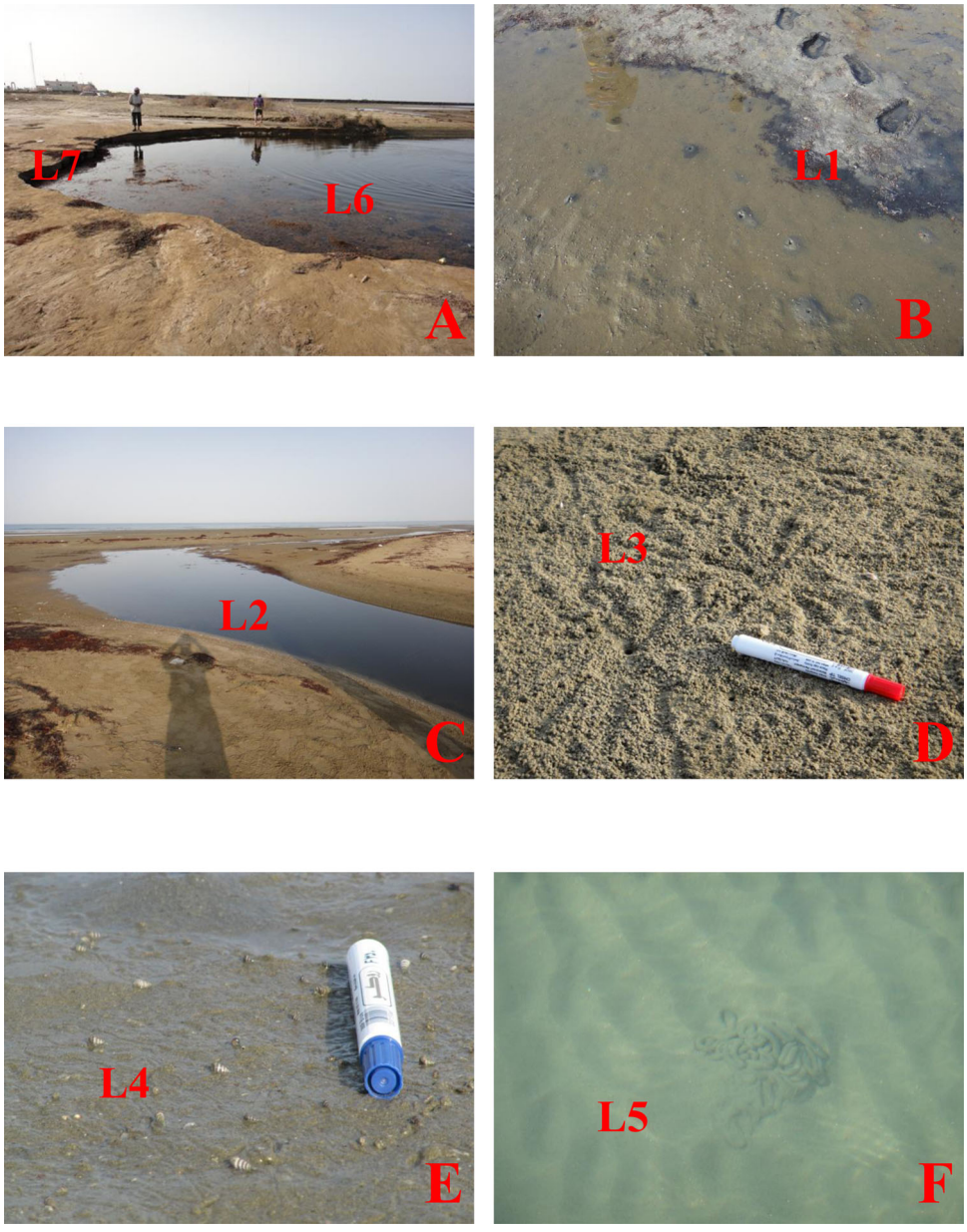

Figure 4. Locality of samples collected for this study: Four clay to fine sand samples (L1 through L4) from tidal flats close to the shoreline and two clay samples (L6 and L7) from a small pond with abundant algae. Sample L5 is subtidal mud collected 100 m from the coastline at 1.5 m water depth. Figure 3(a) (the pond) is farthest (about 150 m) from the shoreline; Figures 3(b–e) approach the shoreline in alphabetical order. Figure 3(f) is located in the sea at 1.3 m water depth about 100 m from the shoreline.

L1: Black mud from a small pond on the tidal flat (Figure 3(b))
L2: Tidal channel that connects the pond (Figure 3(a)) with the sea (Figure 3(c))
L3: Tidal flat surface, full of fecal pellets and bioturbation (Figure 3(d))
L4: Tidal flat along the shoreline (Figure 3(e))
L5: Subtidal mud, 100 m from the coast at 1.3 m water depth (Figure 3(f))
L6: Mud and fine sand from the middle of the pond (Figure 3(a))
L7: Silty to sandy laminated sediment on the edge of the pond (Figure 3(a))

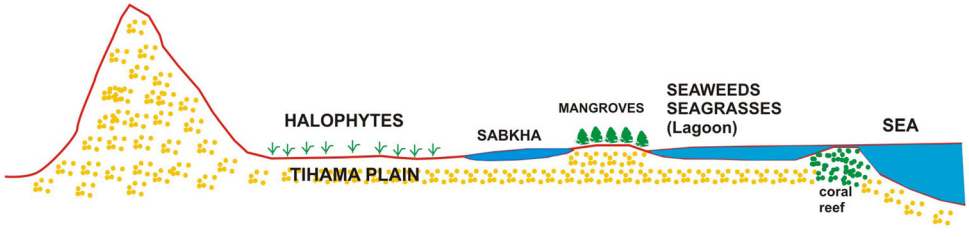

Figure 5. A generalised geomorphological cross-section of the Red Sea coast of Saudi Arabia showing various environments and plant communities (modified after Saifullah 1994).

clay to fine sand samples (L1 through L4) were taken from different areas of tidal flats close to the shoreline, and two clay samples (L6 and L7) came from a small pond with abundant algae. The pond is located 150 m from the shoreline, making samples L6 and L7 the farthest inland from the coastline. Sample L5 is subtidal mud collected 100 m from the coastline at 1.5 m water depth (Figures 3 and 5).

Sample lithology and locations are as follows: L1 is black mud from a small pond on the tidal flat (Figure 3(b)); L2 is from a tidal channel that connects the pond (Figure 3(a)) with the sea (Figure 3(c)); L3 is from a tidal flat surface full of fecal pellets and bioturbation (Figure 3(d)); L4 is from a tidal flat along the shoreline (Figure 3(e)); L5 is from subtidal mud, 100 m from the coast at 1.5 m water depth (Figure 3(f)); L6 is mud and fine sand from the middle of the pond (Figure 3(a)), and L7 is silty to sandy laminated sediment from the edge of the pond (Figure 3(a)).

One cubic centimetre (cm^3) of each sample was used in the maceration process, using standard palynological methods as follows: (1) treatment with 10% hydrochloric acid (HCl) for 15 minutes to remove carbonates; (2) overnight cold hydrofluoric acid (HF, 40%) treatment to remove silicate minerals; (3) treatment with commercial grade nitric acid (HNO_3, sp. gr. 1.35) for 2 hours at 80 °C for oxidation of organic matter, to remove unwanted organic debris; (4) treatment with 10% potassium hydroxide (KOH) for 15 minutes followed by rotation at 1000 rpm for 5 minutes to remove humic matter; (5) treatment of solution with 5% HCl to neutralise pH; (6) residue sieved through 10-μm nylon sieve to remove clay minerals; (7) residue with fraction larger than 10 μm mixed thoroughly with 3 drops of polyvinyl alcohol, smeared over a coverslip and dried at 60 °C over a hot plate; (8) coverslip mounted on a slide with Canada Balsam and kept for 20 minutes over the hot plate at 80 °C. Four slides of each sample were made.

The slides were studied under an OMAX Optical Microscope (MD827S30L Series) using transmitted light. Each slide was scanned under ×400 magnification and palynomorphs were photographed at ×400 and ×1000 (oil immersion) using the microscope's built-in camera system. A few very large palynomorphs were photographed at ×100 as well. Since palynomorph numbers are generally low, all palynomorphs in each slide were counted. Samples yielded low numbers but a high diversity of palynomorphs. The majority of the recovered palynomorphs are illustrated in Plates 1–6 to show the taxonomic diversity in various samples.

Results and discussion

Various types of palynomorphs having diverse affinities and origins were observed in this study. They have been divided into five groups: (A) pollen and spores; (B) dinoflagellate cysts and algal remains; (C) fungal spores, hyphae and fruit bodies; (D) protists and invertebrate remains; and (E) miscellaneous and unidentified forms.

A. Pollen and spores

A total of 21 pollen taxa (18 angiosperms and three gymnosperms) and five spore taxa were observed in this study (Plate 1; Table 1). There is no published pollen atlas of Saudi Arabian plants. However, there are several publications on the palynology of Quaternary and Recent sediments in and around the Arabian Peninsula that describe both pollen and NPP. A few of them describe and illustrate the morphology of common Recent pollen and spores (El-Naggar and El-Husseini 2001; Kholeif 2007; Al-Dabbas et al. 2010; Awadh et al. 2010; Shamso and Toshiyuki 2012). Other publications describe and illustrate a few pollen along with NPP (Kholeif 2004; Al-Ameri and Jassim 2009; Matsuoka et al. 2017). These papers helped in identifying certain pollen and spores. Information on floral compositions of various vegetation types in Saudi Arabia from Thomas (2011) is used here to discuss the provenance of several pollen types found in these assemblages.

Although pollen and spores form only a minor constituent of the palynomorph assemblages, rare occurrences (1–4 specimens) of 18 angiosperm pollen taxa, three gymnosperm pollen taxa, and five spore taxa were observed (see Tables 1 and 6). Among the angiosperms, the monocotyledonous family Arecaceae (syn. Palmae) is represented by the largest number of taxa; they are *Neocouperipollis* sp., *Palmaepollenites* sp., *Palmidites* sp. *Spinizonocolpites* sp. (Nypa palm), *Trichotomosulcites* sp. and *Verrualetes* sp. According to website 1, four palm species occur in Saudi Arabia; they are *Hyphaene thebaica*, *Phoenix caespitosa*, *Phoenix dactylifera* and *Phoenix reclinata*. The date palm (*Phoenix dactylifera*) is an important crop in Saudi Arabia. This family also contains commercial species such as coconuts, areca nuts and date palms, and many indoor and ornamental species as well. The Arecaceae pollen taxa reported in this assemblage probably belong to these species of palms and were transported by wind (sand and dust storms) and water (flash floods and rains) from the neighbouring regions and beyond, since various species of palms occur widely in the Arabian region and northeast Africa.

Acaciapollenites sp., *Euphorbia* sp., unidentified tricolpate pollen and Chenopodiaceae/Amaranthaceae pollen are other significant pollen taxa of the assemblage. Most of them were derived from the vegetation of the coastal plains, sabkhas and wadis, characterised by low sand dunes and saline marshes. These environments are inhabited by open, drought-deciduous thorn woodlands, mangroves, halophytes, open xeromorphic grasslands and thorn woodlands. The mangrove pollen *Avicennia marina* and *Rhizophora mucronata* are found in this assemblage.

Cyperaceae pollen and pollen of *Artemisia* sp. and *Calligonum* sp. are probably derived from open xeromorphic grasslands, where *Artemisia monosperma* and *Calligonum comosum* are common shrubs of the sand dunes. All these shrubs co-occur with perennial herbs and grasses such as *Cyperus conglomeratus*.

The presence of a single pollen of cf. *Casuarina* sp. is problematic, because it is not native to this area, but *Casuarina* trees planted near Dammam along the Arabian Gulf coast of Saudi Arabia were observed (A. Kumar, personal

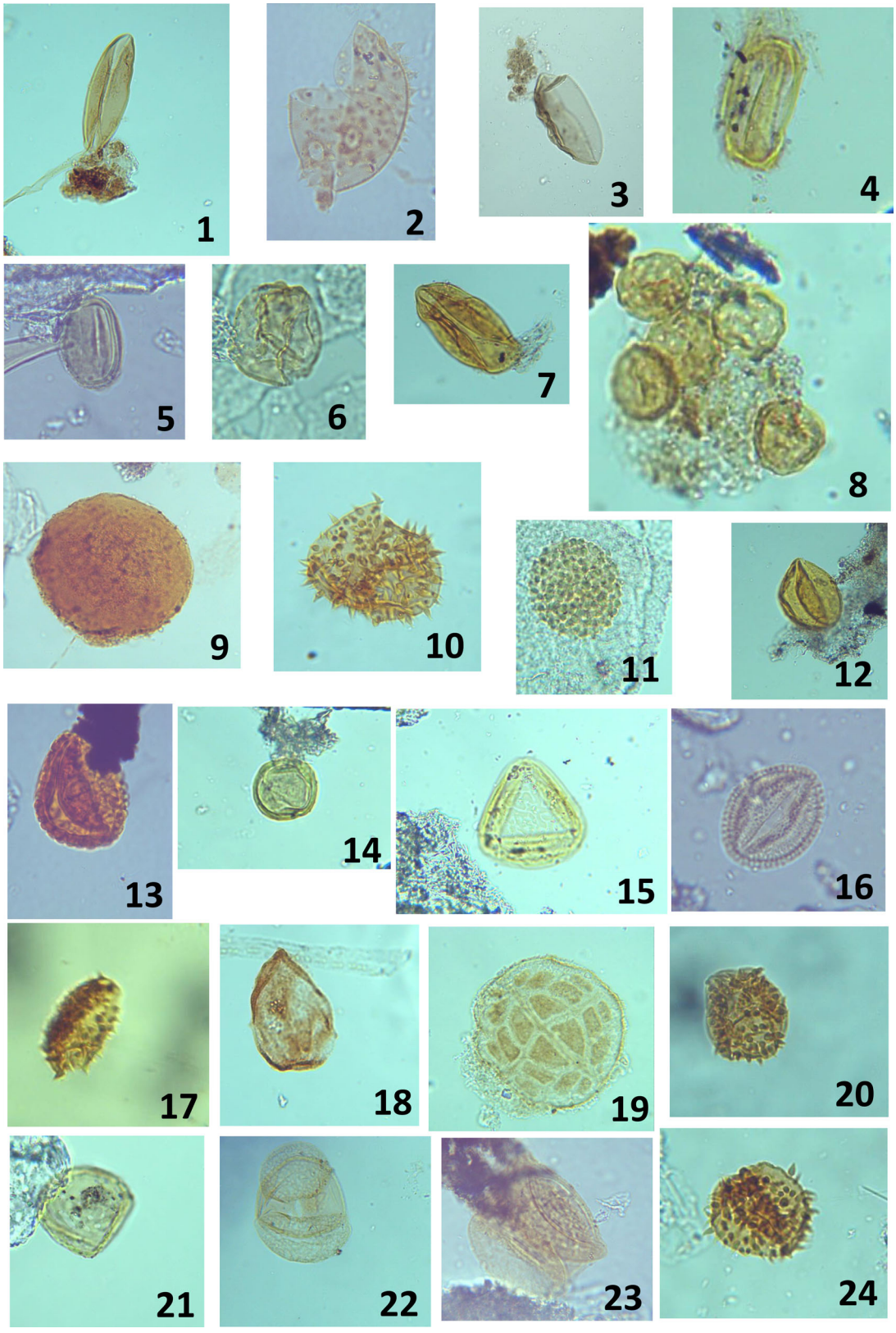

observation). Most likely the *Casuarina* pollen was transported to the study area during thunderstorms or dust storms, which are common in this region.

The presence of cf. *Potomogeton* pollen in this assemblage is problematic, because it is a pond weed that occurs in submerged aquatic habitats. At present there are only rare ponds along the Tihama Plain in this desert environment where *Potomogeton* could grow. Although Saudi Arabia does not have rivers or perennial streams, its seasonal streams and ponds do contain a few species. The aquatic flora in Saudi Arabia contains more than 40 aquatic or semi-aquatic species, of which Potamogetonaceae has the highest number

of species (Thomas 2011). Formation of ponds occurs during flooding events caused by thunderstorms, in which heavy to very heavy rainfall occurs within a short period of time (Kumar 2013). A species of *Potomogeton* might have grown in one such pond contributing to the pollen assemblage.

Among the gymnospermous pollen, *Juniperus* sp., *Pinuspollenites* sp. and *Podocarpus* sp. were observed. The *Juniperus* sp. pollen is related to *Juniperus procera*, which inhabits higher altitudes in the southwestern parts of the Arabian Peninsula. *Pinus* and *Podocarpus* are not known in the Arabian region. However, *Pinus* and *Podocarpus* pollen were reported from Pleistocene and Holocene sediments of the Nile Cone, Egypt (Kholeif and Mudie 2009).

Pinus is a genus of the family Pinaceae; it has characteristic bisaccate pollen. This family is distributed worldwide including in North Africa. *Pinus radiata* was introduced in sub-Saharan Africa for timber production, and *Podocarpus* is known from the tropical highlands of Africa. Tropical cyclones originating in the Arabian Sea are known to impact the Arabian Peninsula, mainly in the southern regions such as Yemen and Oman. Pollen of *Pinus* and *Podocarpus* were most likely transported from East Africa by these cyclones or the southwest monsoon, when the summer wind blows across the Arabian Sea from northeast Africa to India with a branch that veers north towards the Arabian Peninsula.

Five taxa of pteridophytic spores were observed that belong to the fern families Lycopodiaceae and Polypodiaceae. In Saudi Arabia there are 27 species of pteridophytes. They occur in most terrestrial habitats and in some aquatic communities. The observed spore taxa must be related to these plants and were most likely transported by both wind and water to the site of deposition.

B. Dinoflagellate cysts and algal remains

The following dinoflagellate cysts and algal remains were identified.

B1. Dinoflagellate cysts

Three known and six unknown dinoflagellate cyst taxa were found in this study (Tables 2 and 6). The unknown taxa are described here.

Dinoflagellate cyst A (Plate 2, figure 1). Large, antero-posteriorly compressed cyst. The epicyst and hypocyst are featureless; with an apical notch. The cingulum and sulcus are not evident; with psilate autophragm. There is a large archaeopyle; based on its shape, it could be intercalary.

Cyst diameter 62 μm (one specimen).

Dinoflagellate cyst B (Plate 2, figure 2). An elongated, light brown, acavate, peridinioid cyst, autophragm thin, psilate and wrinkled. Paratabulation features are not distinct except for a faint sulcus. There is an opening in the epicyst but the nature of the archaeopyle is not certain. It has a distinct apical horn and two short antapical horns.

Cyst size 87 × 57 μm (two specimens).

Dinoflagellate cyst C (Plate 2, figure 3). A large proximate cyst; dorso-ventrally compressed and of peridinoid shape, with a short apical and two short antapical horns. Autophragm psilate; paratabulation is indicated clearly only by a distinct cingulum and sulcus. The archaeopyle is not distinct but there is an undefined opening in the epicyst; thus, it is difficult to infer the nature of the archaeopyle.

Cyst size 109 × 97 μm (one specimen).

Dinoflagellate cyst D (Plate 2, figure 4). Proximate, subspherical, acavate cyst. Autophragm psilate to faintly microreticulate; paratabulation is indicated only by an apical archaeopyle with free operculum.

Cyst size 48 × 44 μm (one specimen).

Dinoflagellate cyst E (Plate 2, figure 12). Proximate, elongate-subspherical, acavate cyst. Autophragm thin, psilate and wrinkled, pale brown in colour; paratabulation is indicated only by an apical archaeopyle with an attached operculum.

Cyst size 72 × 48 μm (one specimen).

Dinoflagellate cyst F (Plate 2, figure 15). Small sub-rectangular cyst with compound epicystal archaeopyle. Autophragm psilate with tubercles. Processes are reduced and very short.

Cyst diameter 31–37 μm; archaeopyle 21–23 μm (two specimens).

These forms are mostly thin walled and do not always show complete dinoflagellate cyst-like paratabulation characters except for their shape, thin and generally psilate

Plate 1. All photos ×400 unless otherwise mentioned. 1. *Palmaepollenites* sp. (Arecaceae); slide L3a; 9 × 146.5; size 69 × 23 μm. 2. *Nypa* sp. (Arecaceae); slide L3d; 5 × 139; size 59 × 40 μm; spines (L) 2–3 μm (W) 1.5–2 μm (×1000). 3. *Palmidites* sp. (Arecaceae); slide L2b; 7.2 × 147.4; size 72 × 34 μm. 4. Tricolpate psilate pollen (Dicotyledonae); slide L3d; 13.2 × 151.5; size 32 × 17 μm. 5. cf. *Avicennia marina* (Avicenniaceae); slide L6a; 14 × 154.2; size 24 × 17 μm (×1000). 6. ? *Casuarina* sp. (Casuarinaceae); slide L2d; 4 × 155; size 50 × 38 μm Not native to the area but planted in the eastern part of the Kingdom of Saudi Arabia). 7. *Palmaepollenites* sp. (Arecaceae); slide L3c; 2.3 × 143.5; size 56 × 27 μm. 8. A cluster of Chenopodiaceae/Amaranthaceae pollen; slide L6c; 3 × 145.8; size 13–15 μm. 9. cf. *Potamoegeton* sp.; slide L3c; 14 × 151.5; size 86 μm. 10. *Nypa* sp. (Arecaceae); slide L2a; 8.8 × 162.5; size 34 × 26 μm; spines (L) 2–3 μm; (W) 1–1.5 μm (×1000). 11. *Verrualetes* sp. (Arecaceae); slide L7a; 16.5 × 136; size 39 μm. 12. *Calligonum* sp. (Polygonaceae); slide L2d; 17 × 164; size 52 × 38 μm. 13. *Euphorbia* sp. (Euphorbiaceae).; slide L3c; 5.8 × 131.6; size 45 × 33 μm; verrucae 1.5 × 2.0 μm (×1000). 14. *Rhizophora mucronata* (Rhizophoraceae); slide L5b; 13.3 × 138.2; size 29 × 24 μm (×1000). 15. *Trichotomosulcites* sp. (Arecaceae); slide L6d; 5.6 × 147.5; size 54 × 50 μm. 16. *Artemisia* sp.; slide L4b; 16.2 × 156; size 18 μm (×1000). 17. *Neocouperipollis* sp. (Arecaceae); slide L2d; 18.5 × 156.6; size 38 × 18 μm; spines (L) 2.5–3 μm; (W) 1–1.5 μm. 18. Cyperaceae pollen; slide L1b; 167 × 12; size 41 × 35 μm. 19. *Acacia* sp. (Leguminosae); slide L2a; 12 × 152.5; 45 μm. 20. *Neocouperipollis* sp (Arecaceae); slide L3c; 2 × 150.5; size 33 × 30 μm; spines (L) 2–3 μm; (W) 1–1.5 μm. 21. Chenopodiaceae/Amaranthaceae pollen; slide L3c; 19 × 127; size 39 μm. 22. *Pinus* sp. (Pinaceae); slide L3a; 5 × 162; size: body 43 × 42 μm; sacs 37 × 31 μm. 23. *Podocarpus* (Podocarpaceae); slide L6c; 9.5 × 150; size: body 38 × 17 μm; sacs 42 × 20 μm (×1000). 24. *Neocouperipollis* sp. (Arecaceae); slide Lc6; 5 × 143.5; size 31 μm, spines 2.5–3.0 μm.

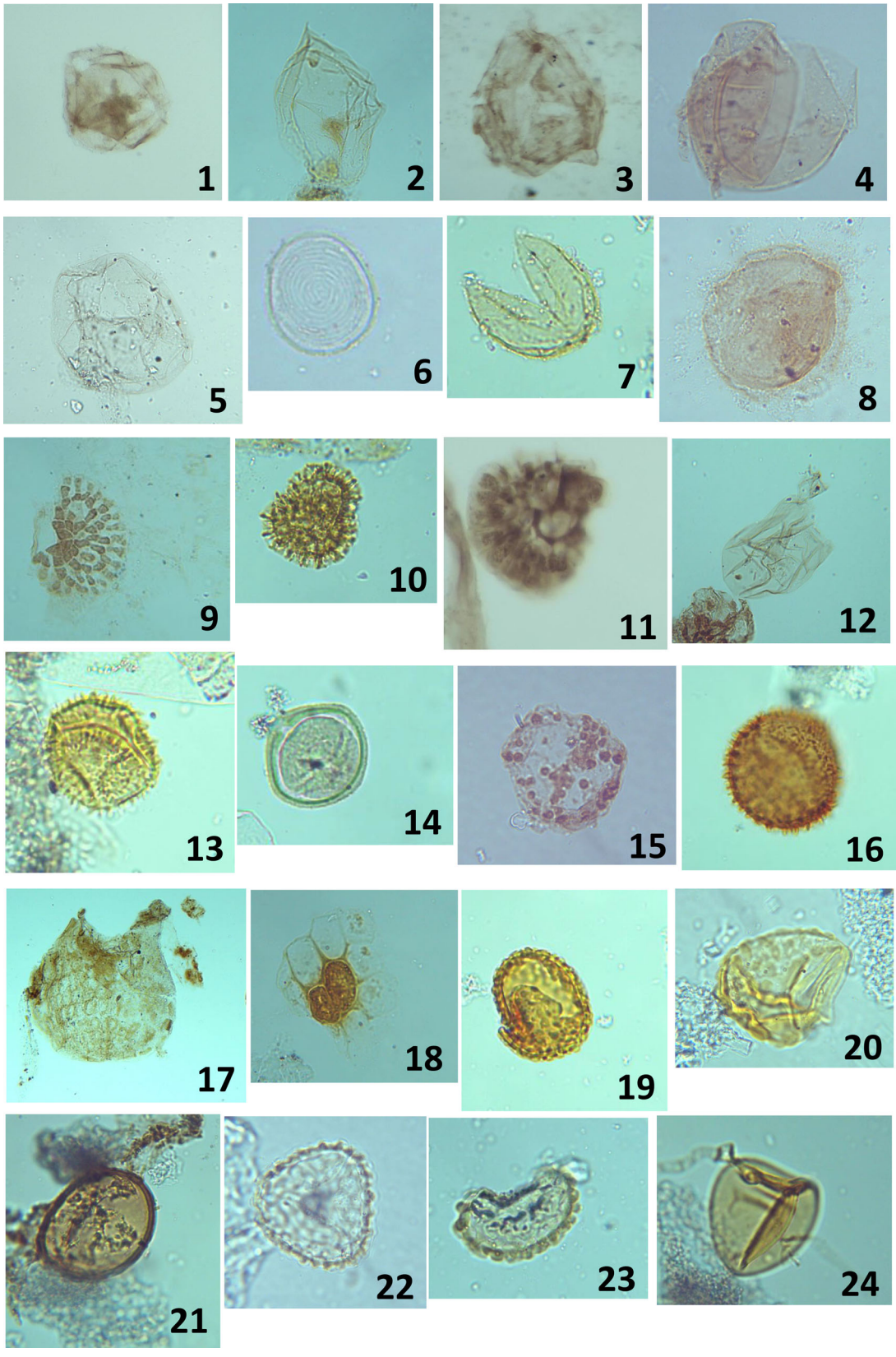

autophragm and archaeopyle. It is difficult to compare them with any known dinoflagellate cyst because of their poor preservation and lack of morphological features that could be useful for any meaningful comparison. The six unknown dinoflagellate cysts (types A, B, C, D, E and F), found only as one or two specimens each, appear to have morphological affinities with fresh- and brackish-water dinoflagellate cysts.

Only a few dinoflagellate cyst taxa were observed; they appear to be a mix of fresh- or brackish-water forms along with marine forms from the coastal lagoons of the Red Sea. Freshwater dinoflagellates are characteristically thin walled,

and often the archaeopyle is not visible, due to poor preservation or because it might be hidden by folds in the autophragm. Furthermore, paratabulation features are either not well developed or not identifiable (Cole 1992). Fresh- to brackish-water dinoflagellate cysts typically are of smaller size and of simple proximate shape, and have a thin autophragm; they occur with low species richness but have a high dominance in the assemblages. They are often associated with tidal channel and tidal mudflat facies that provide evidence of a possible upper estuarine setting (Wainman et al. 2019). There are approximately 350 freshwater dinoflagellate species, and 84 resting cyst species; their shapes, wall ornamentations, archaeopyles and colours are important morphological characteristics at the generic level (Mertens et al. 2012).

The dinoflagellate cyst assemblage observed in this study is largely marine (?*Operculodinium* sp.; spiny round brown cyst (SRBC) with theropylic archaeopyle but also includes some freshwater forms, especially *Peridinium* sp. Resting cysts attributed to the freshwater dinoflagellate genus *Peridinium* sp. have been described from the lakes of North America (McCarthy et al. 2011, 2018; Krueger and McCarthy 2016).

B2. Algal remains

There are no published accounts of any algal remains from the Red Sea coastal sediments. The closest such accounts are from Egypt (Kholeif and Mudie 2009; Elshanawany et al. 2010). Like pollen and spores, dinoflagellate cysts and algal remains are a minor constituent of the palynomorph assemblages; only rare (1–4 specimens) occurrences were observed (Tables 2 and 6).

Long slender filaments, generally septate, branched or unbranched, are found commonly in most samples. Thin-walled spherical cysts with psilate or scabrate, intact or broken walls, usually ranging between 25 and 40 μm, are common. Some were attributed to algal cell types A and B, while others were recorded as 'algal cyst (unidentified)'. A total of 11 algal forms are recorded (Tables 2 and 6).

Botryococcus, *Concentricystis* and *Spirogyra* zygospores, *Lecaniella* (*Spirogyra* zygospores), Cyanobacteria *Gleotrichia* sp. and *Rivularia* are the other algal remains found in the present assemblages.

Botryococcus is a colonial green alga of the order Chlorococcales that tolerates variable salinities, thus inhabiting brackish or freshwater environments including ponds and temporary pools, and found in temperate to tropical oligotrophic lakes and estuaries (de Vernal 2009).

Concentricystis is another algal spore found in freshwater habitats, in the form of zygospores of spheroid to obovoid shape, which have a hyaline, ornamented wall with concentric rings in polar view. It is indicative of freshwater marshy environments. It is also known as *Pseudoschizaea* (Limaye et al. 2007).

Cyanobacteria or blue-green algae normally occur in lakes and ponds. *Gleotrichia* sp. is a cyanobacterium that indicates freshwater input in brackish water conditions (Limaye et al. 2007; Kumaran et al. 2008), thus indicating a brackish-water, littoral environment.

Rivularia is a modern cyanobacterium belonging to the family Rivulariaceae, order Nostocales. It grows on plants and can also be free-floating and photosynthetic, and becomes abundant when there is an incursion of saltwater; thus, its abundance could be a proxy for a brackish-water, littoral environment (Limaye et al. 2007; Kumaran et al. 2008).

Lecaniella is a *Spirogyra* zygospore. *Spirogyra* is a filamentous chlorophyte or green alga of the order Zygnematales and is commonly found in freshwater habitats. According to Hoshaw and McCourt (1988), 'Zygospores (resting, encysted zygotes of some chlorophyte algae) are often produced during seasonal dessication of the habitat, and changes in water chemistry (nitrogen depletion and rise in pH) and light regime seem to be responsible for triggering zygospore formation'. Seasonal desiccation of habitat and changes in water chemistry in the Red Sea coastal ponds occur annually, and may be when the *Spirogyra* zygospores formed (Head 1993).

Thus, it is evident from the dinoflagellate cysts and algal remains that these assemblages contain a mixture of freshwater or brackish and marine forms. This interpretation is confirmed by the presence of microforaminifera and thecamoebians in these assemblages.

C. Fungal spores, hyphae and fruit bodies

Fungal spores and hyphae occur commonly in most of the samples. Fungal fruit bodies and spores have been identified as belonging to 12 fungal taxa (Plate 3; Tables 3 and 6).

Fungi, unlike many groups of plants, have no chlorophyll; they are heterotrophs and survive as epiphytes, saprophytes or parasites, or in symbiotic associations on or in living or dead plants and animals. They rarely produce hard resistant tissues and are thus not prone to fossilisation; however, their spores, hyphae and fruit bodies are preserved as organic matter and can be isolated using palynological maceration techniques

Plate 2. All photos ×400 unless otherwise mentioned. 1. Dinoflagellate cyst A; slide L1.; 15.5 × 132.7; size 62 μm. 2. Dinoflagellate cyst B; slide L1a; 4.5 × 140.5; size 87 × 57 μm. 3. Dinoflagellate cyst C; slide L1a; 7 × 154.5; size 109 × 97 μm. 4. Dinoflagellate cyst D; slide L2a; 10 × 155; size 48 × 44 μm (×100). 5. *Peridinium* sp.; slide L2a; 8 × 148.4; size 88 × 81 μm. 6. *Concentricystis* sp. slide L6d; 2 × 148.5; size 30 μm. 7. *Lecaniella* sp. (*Spirogyra* zygospore); slide L5c; 13 × 132.7; size 42 μm. 8. Resting egg of *Artemia* brine shrimp; slide L2b; 16.5 × 159; size 108 × 78 μm (×1000). 9. Colonial alga/Cyanobacteria; slide L1a; 5 × 145.5; size 69 × 55 μm. 10. Algal cyst (unidentified); slide L2c; 21.5 × 150; size 31 × 26 μm; processes 3–3.5 μm. 11. *Botryococcus* sp.; slide L1b; 14.5 × 152.2; size 40 μm. 12. Dinoflagellate cyst E; slide L3a; 7.6 × 139.5; size 72 × 48 μm. 13. ?*Operculodinium* sp.; slide L5c; 11.5 × 128.5; size 28 μm; processes 1.5 μm. 14. Algal cell type A; slide L5d; 3.2 × 137; size 29 μm. 15. Dinoflagellate cyst F; slide L6c; 11.5 × 160; size 31 μm; archaeopyle 21 μm. 16. Spiny Round Brown Cyst (SRBC); slide L2d; 13.5 × 149.5; size 30 μm; processes 1.5–2 μm (×1000). 17. Algal body (unidentified); slide L3a; 12.3 × 145.5; size 240 μm (×1000). 18. Algal cells type B; slide L3d; 3.5 × 137; size 28 × 17 μm; processes 10–14 μm. 19. *Juniperus* pollen; slide L6c; 14.5 × 151.5; size 34 × 24 μm; verrucae 1–1.5 μm. 20. *Verrucosisporites* sp. (Polypodiaceae); slide L6c; 13.5 × 141; size 38 μm; verrucae 2–3 μm (×1000). 21. *Laevigatosporites* sp. (Polypodiaceae); slide L6d; 6.5 × 133.6; size 58 × 47 μm. 22. *Lycopodiumsporites* sp. (Lycopodiaceae); slide L6b; 9 × 140; size 39 μm (×1000). 23. *Polypodiisporites* sp.; slide L6a; 13.5 × 126; size 49 × 23 μm; gemma 2.5–3 μm. 24. *Triplanosporites* sp.; slide L6d; 12 × 158; size 43 × 41 μm.

(Kalgutkar and Jansonius 2000). Elsik (1996) and Kalgutkar and Jansonius (2000) provide a comprehensive account of the diverse aspects of palaeomycology, i.e. the study of fossil fungal palynomorphs including morphology, descriptive terminology, identification and nomenclature, geological history, palaeoenvironmental and palaeoclimatic significance, etc.

In the present assemblages, few (5–10 specimens) to common (11–25 specimens) fungal remains representing fungal spores, hyphae, fruit bodies and several unidentified fungal forms are found in the samples (Tables 3 and 6). Fungal hyphae and *Callimothallus*-type fruit bodies are abundant (51 or more specimens) in sample L1. Unidentified fungal remains are common in all samples. Fungi provide evidence for relative humidity, atmospheric pressure and precipitation rates. Assemblages of fungal spores in higher diversity and numbers are usually considered to be indicative of warm and humid climatic conditions (Limaye et al. 2007; Kumaran et al. 2008).

Glomus sp. (family Glomeraceae) is an endomycorrhizal fungus showing a symbiotic relationship with roots of higher plants. These are globose chlamydospores, aseptate and inaperturate, and are of variable size (18–138 μm). *Glomus* chlamydospores form below the soil surface and are not normally transported (Cook et al. 2011). In postglacial sediments in Maine, USA, their increase during the late glacial indicated increased soil erosion, and their decline during the Holocene accompanied increased soil stability. Thus, they are indicative of soil erosion in the catchment area (Anderson et al. 1984). In Australia, *Glomus* was found to be a useful indicator of soil erosion in the catchments of two lakes (Cook et al. 2011). This fungal spore provides a useful line of palaeoecological evidence.

Fungal fruit bodies (Microthyriaceae) are multicellular, epiphyllous forms; they occur most likely on the coastal mangrove stands and are indicative of tropical to subtropical moist humid climate and heavy rainfall. There are several types of flattened fruit bodies referable to *Trichothyrites*, *Callimothallus* and *Phragmothyrites* (Limaye et al. 2007; Kumaran et al. 2008), and all of them occur in the present assemblages. Fungal hyphae are unicellular to multicellular, branched or unbranched forms that occur primarily in freshwater marsh/floodplain environments and are indicative of high organic input and heavy rainfall. Fungal spores are unicellular or multicellular, septate or aseptate and with or without pores, and occur in the present assemblages.

The present assemblage of fungal remains is indicative of dry, hot and brackish coastal environments that periodically become wet and humid due to short-term excessive rainfall during tropical storms.

D. Protists and invertebrates

Three groups of protists are present in the assemblages of this study: foraminifers, thecamoebians and tintinnids. Benthic foraminifers are quite ubiquitous in brackish/marine environments ranging from intertidal zone to deep oceans, and are present from the polar regions to the tropics as microforaminiferal test linings. Thecamoebians are also known as agglutinated rhizopods or testate amoebae; they are benthic microfauna that occur worldwide in bodies of fresh and brackish water. Tintinnids are present as tintinnomorphs that are part of the microzooplankton, inhabiting primarily marine waters, but brackish and fresh water as well.

D1. Microforaminiferal test linings

Microforaminiferal test linings are the inner organic remnants of the benthic microforaminifera, commonly observed in palynomorph assemblages of marine and brackish-water sediments. They are acid-resistant, chitinoid linings, usually <150 μm in size. Microforaminiferal test lining types 1 through 7 were identified; their distribution is shown in Tables 4 and 6. These linings have been used as proxies for water pollution, ocean productivity and palaeoenvironmental studies (Stancliffe 1996).

Mudie and Yanko-Holmbach (2019) carried out concurrent palynological and micropalaeontological studies to investigate the relationship between the morphology and abundance of these linings and benthic foraminiferal assemblages along transects off the Danube River Delta, northwest Black Sea. They made paired comparisons of the morphology, abundance and preservation state in test linings and foraminiferal assemblages at 17 sites along a surface-water salinity gradient from the delta front to the outer shelf.

Monga et al. (2015) used several chambers and the size of the linings to define various groups of microforaminiferal linings, as Uniserial type II, Biserial type II, Planispiral type II, Planispiral type III, Planispiral type IV, Trochospiral type I and Trochospiral type II. These groups were used to delineate marine and terrestrial realms in the Paleogene sequences and facilitated better interpretation of the depositional environment. Microforaminiferal linings provide a means of reconstructing the nature of marine-influenced depositional settings.

Mathison and Chmura (1995) developed a qualitative classification of the physical condition of microforaminiferal test linings based on whether individual chambers were intact or damaged (split or torn), and whether they were closely spaced (proximate) or if the spacing of the individual chamber was open. Based on these criteria, seven microforaminiferal linings from the present study can be described as follows. None of the specimens have any torn or split chambers.

Type 1: brownish, trochospiral, proximate; size 64 μm (Plate 6, figure 11);
Type 2: brownish, planispiral, proximate; size 61 μm (Plate 6, figure 12);
Type 3: brownish, trochospiral, proximate; size 104×74 μm (Plate 6, figure 13);
Type 4: brownish, trochospiral, open; size 105×66 μm (Plate 6, figure 14);
Type 5: brownish, trochospiral, open; size 73×51 μm (Plate 6, figure 15);
Type 6: yellow, planispiral, proximate; size 95×77 μm (Plate 6, figure 16);
Type 7: light grey, uniserial, open; size 114×70 μm (Plate 6, figure 17).

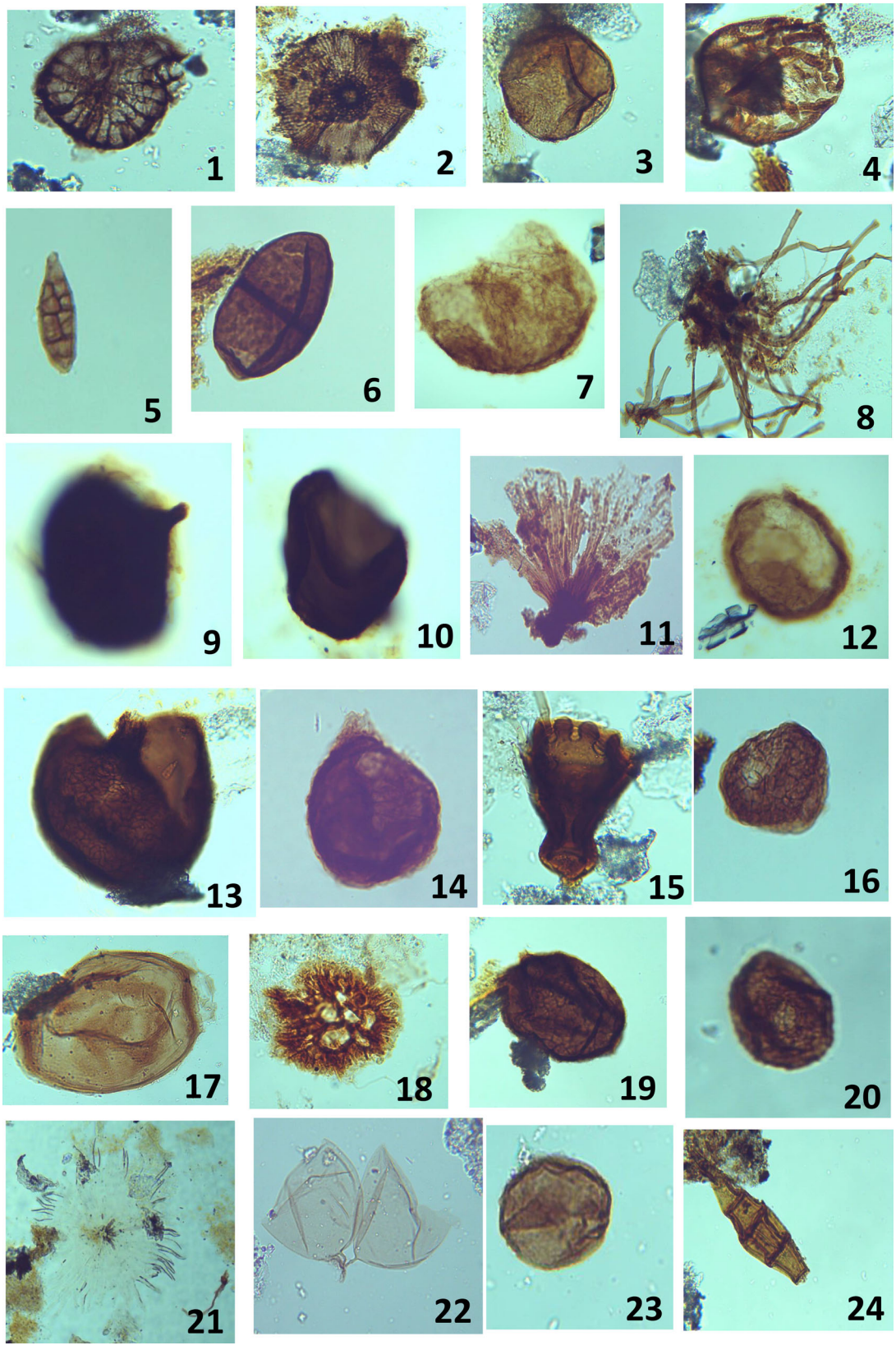

Plate 3. All photos ×400 unless otherwise mentioned. 1. *Phragmothyrites* sp.; slide L4a; 20.5 × 161; size 60 × 50 μm. 2. *Trichothyrites* sp.; slide L4b; 4 × 161.5; size 93 × 76 μm. 3. *Inapertisporites* sp.; slide L4c; 13.5 × 147.3; size 71 × 64 μm. 4. Fungal sporangium containing hyphae and spores; slide L4d; 10.6 × 145; size 72.5 μm. 5. *Diporicellaesporites* sp.; slide L1c; 22.5 × 137; size 27 × 10 μm. 6. *Dicellaesporites* sp.; slide L3c; 18 × 135.3; size 65 × 38 μm. 7. *Dictyosporites* sp.; slide L1c; 20.2 × 136.7; size 142 μm. 8. Fungal hyphae; slide L2c; 11.2 × 152.2. 9. *Callimothallus* type fruiting body; slide L1c; 13.8 × 139.6; size 132 × 106 μm; horn 18 × 11 μm. 10. *Callimothallus* type fruiting body; slide L1c; 11.8 × 165; size 90 × 83 μm. 11. *Rivularia* sp. (Cyanobacteria); slide L6d; 19.5 × 151; size 127 μm. 12. *Dictyosporites* sp.; slide L1c; 12 × 137.5; size 100 × 84 μm. 13. *Callimothallus* type fruiting body; slide L2c; 10 × 159.5; size 120 μm. 14. *Brachysporisporites* sp.; slide L2c; 10 × 164.5; size 42 × 38 μm; ×100. 15. Unidentified fungal remains; slide L6b; 9 × 149.5; size 89 × 65 μm. 16. *Dictyosporites* sp.; slide L1c; 149.5 × 3; size 46 × 41 μm. 17. *Biporipsilonites maximus* (Song & Luo) Kalgutkar and Jansonius 2000; slide L6a; 12 × 131; size 152 × 102 μm. 18. Unidentified fungal remains; slide L1a; 151.7 × 16; size 92 × 75 μm. 19. *Monoporisporites* sp.; slide L3c; 14.3 × 147; size 93 × 67 μm. 20. *Monoporisporites* sp.; slide L3c; 7 × 138.2; size 48 × 37 μm. 21. *Gleotrichia* sp. (Cyanobacteria); slide L2c; 15.8 × 160.5; size 265 μm (×100) (see Limaye et al. 2017; Fig. 2/K). 22. *Glomus* sp. slide L6a; 15 × 132.3; size 58 × 48 μm. 23. *Inapertisporites* sp.; slide L6a; 19.8 × 155.5; size 26 μm. 24. *Multicellites* sp.; slide L6c; 17.2 × 159.5; size 89 × 23 μm.

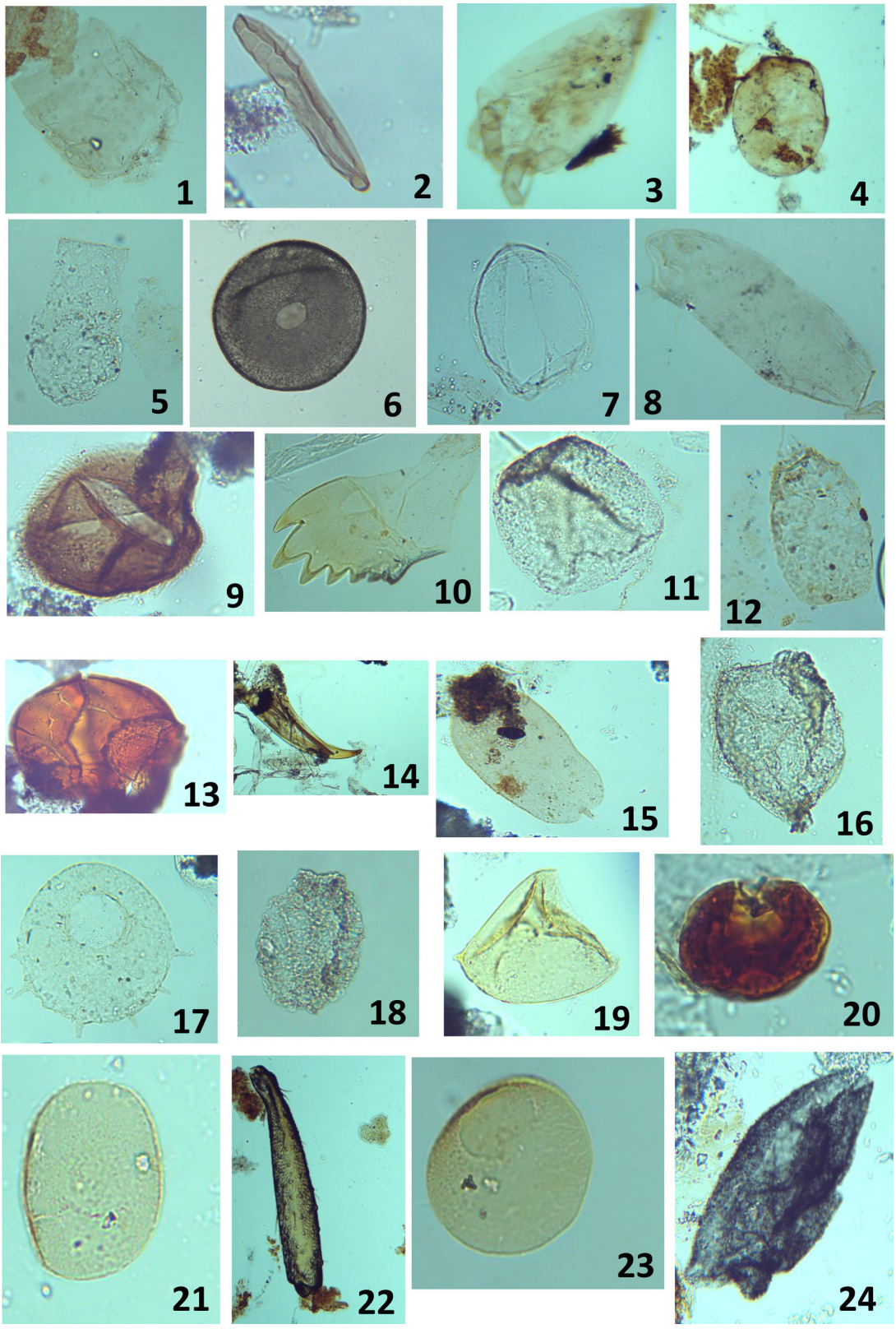

Plate 4. All photos ×400 unless otherwise mentioned. 1. Crustacean thoracic segment (exoskeleton); slide L2a; 15.8 × 152; size 137 × 98 μm; spines (L) 22–20 μm. 2. Small turbellarian worm; slide L5b; 17.2 × 147; size 76 × 14 μm. 3. Insect appendage; slide L1b; 8.5 × 134.8; size 170 × 84 μm. 4. Copepod egg; slide L2b; 18 × 157.5; size 166 × 129 μm (×100). 5. Tintinnomorph type 11; slide L1a; 21.3 × 149; size 88 × 51 μm; opening 31 μm. 6. *Geopyxella sylvicola* Bonnet & Thomas, 1955; slide L2b; 16.5 × 151.5; size (D) μm; aperture (D) 18.5 × 15 μm. 7. Copepod egg; slide L3b; 17 × 157.8; size 85 × 67 μm. 8. Annelid palynomorph; slide L1b; 12 × 154.5; size 140 × 48 μm. 9. Insect part; slide L6a; 4.3 × 151.2; size 79 × 76 μm; hairs 5–7 μm. 10. Ostracod jaw; slide L3d; 14 × 154.5; size 134 × 87 μm. 11. Copepod egg; slide L5c; 11 × 155; size 70 μm. 12. Tintinnomorph type 13; slide L1c; 14.8 × 150.5; size 68 × 43 μm; opening 16 μm. 13. Crustacean head (?); slide L5b; 12 × 140; size 100 × 75 μm. 14. Scolecodont type 1; slide L5c; 14 × 139.2; size 272 × 71 μm (×100). 15. Insect wing; slide L6c; 13.5 × 137; size 90 × 47 μm. 16. Tintinnomorph type 14; slide L2b; 10.4 × 162.2; size 86 × 68 μm. 17. *Centropyxis aculeata*; slide L5c; 17 × 133.5; size (D) 103 × 99 μm; aperture (D) 39 × 35 μm; spine (L) 7–18 μm. 18. Tintinnomorph type 16; slide L5c; 17 × 124; size 62 × 47 μm; opening 18 μm. 19. Tintinnomorph type 15; slide L2c; 15.5 × 158.6; size 60 × 59 μm. 20. Insect exoskeleton; slide L7c; 16 × 138; size 51 × 37 μm. 21. Indeterminate form A; slide L2b; 14.5 × 131.5; size 43 × 33 μm. 22. Crustacean appendage; slide L3a; 3.5 × 144.8; size 380 × 66 μm. 23. Indeterminate form A; slide L3c; 8.5 × 146; size 42 × 38 μm. 24. Copepod egg envelope; slide L4b; 7 × 149.5; size 126 × 48 μm.

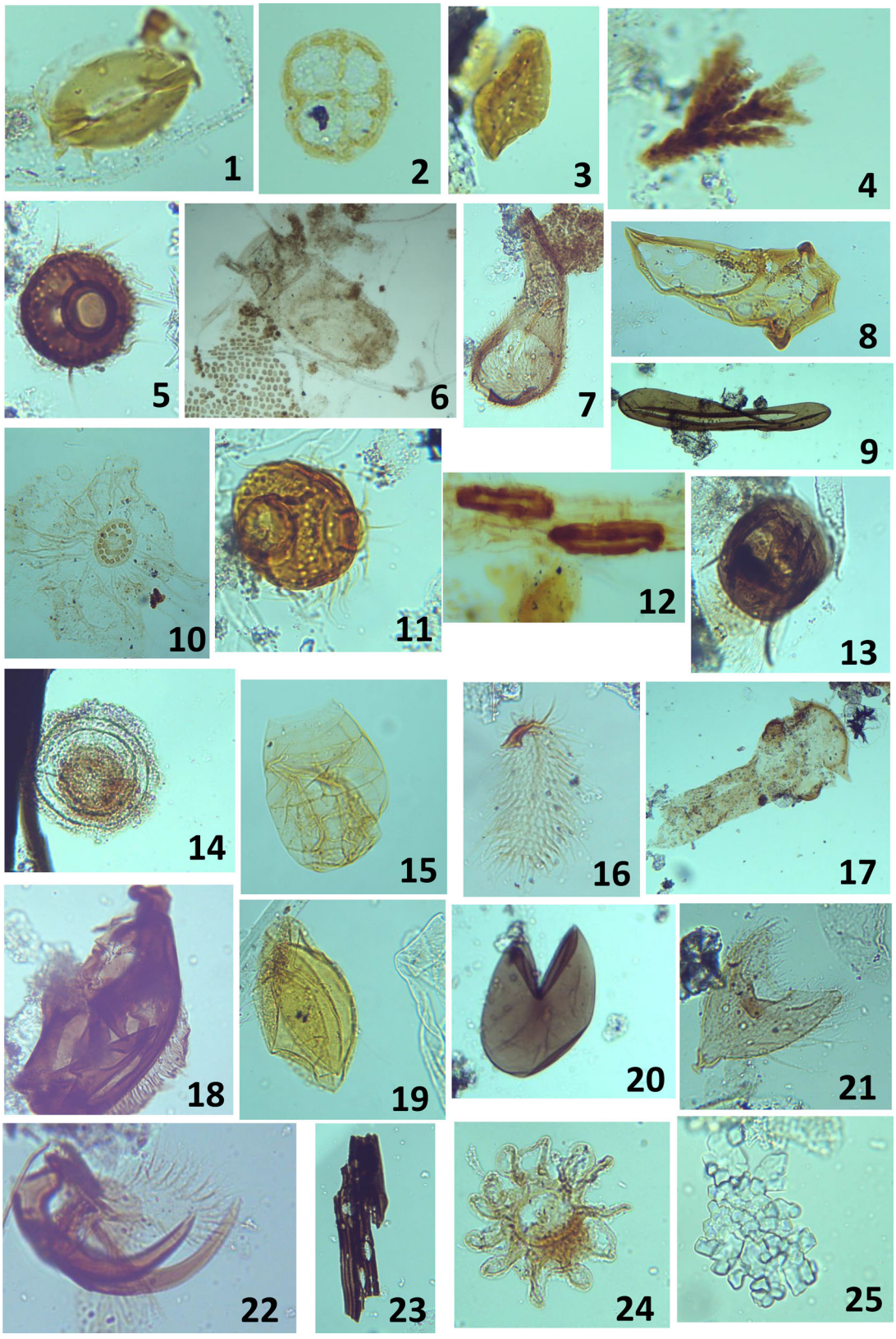

Plate 5. All photos ×400 unless otherwise mentioned. 1. Stomata; slide L2d; 19 × 153; size 42 × 30 μm. 2. Indeterminate Form B; slide L2d; 7.5 × 143.6; size 40 × 34 μm. 3. *Lecaniella* sp. (Zygnemataceous algae zygospore); slide L2d; 16.5.5 × 143.3; size 56 × 29 μm. 4. Crustacean antenna (?); slide L2d; 10.5.5 × 162; size (L) 52 μm. 5. Crustacean head; slide L6a; 9 × 149; size 38 μm; hairs 9–12 μm. 6. Tintinnomorph type 12. slide L1b; 13.7 × 142.6; size 95 × 42 μm; spinules 8–10 μm. 7. Crustacean appendage; slide L6a; 10 × 138 size 146 × 61 μm; hairs 7–10 μm. 8. Annelid jaw; slide L5d; 5.5 × 154; size 132 × 70 μm. 9. Worm; slide L6b; 13.5 × 158; size 358 × 61 μm (×100). 10. Cyanobacteria?; slide L1b; 21.5 × 139; size 36 × 28 μm; processes 60–65 μm. 11. Crustacean head; slide L5c; 4 × 147 size 55 × 50 μm; processes 18–15 μm. 12. Leaf epidermis showing stomata; slide L1c; 12 × 139; size (L) 64 × 71 μm; (W) 21–22 μm. 13. Crustacean head; slide L5d; 5.5 × 158; size 68 × 57 μm; antennae (L)18 μm (maximum). 14. *Pseudoschizaea*/*Concentricystis* sp.; slide L6a; 8.5.5 × 150.5; size 51 μm. 15. Tintinnomorph type 17; slide L3c; 2.2 × 131.7; size 76 × 59 μm. 16. Copepod antenna; slide L6c; 5.3 × 161.8; size 68 × 35 μm; spines 14–23 μm. 17. Annelid remains (?); slide L6b; 7 × 158.6; size 316 × 147 μm (×100). 18. Copepod fragment; slide L6a; 10.5 × 143.5 size 200 × 85 μm. 19. Spirogyra zygospore; slide L5d; 9.5 × 153; size 92 × 50 μm; capsule 73 × 35 μm. 20. Indeterminate form E (Crustacean egg?); slide L6b; 13.5 × 130.2; size 175 × 121 μm. 21. Copepod antenna; slide L6b; 21 × 148.5; size 74 × 49 μm; processes 35–25 μm. 22. Scolecodont type 2; slide L6a; 21.3 × 140; size 68 × 11 μm. 23. A piece of charcoal; slide L7a; 22 × 147; size 96 × 27 μm. 24. Algal cyst?; slide L2a; 15.2 × 155; size 63 × 60 μm. 25. Phytoliths; slide L6d; 9.5 × 132; size 45 × 41 μm.

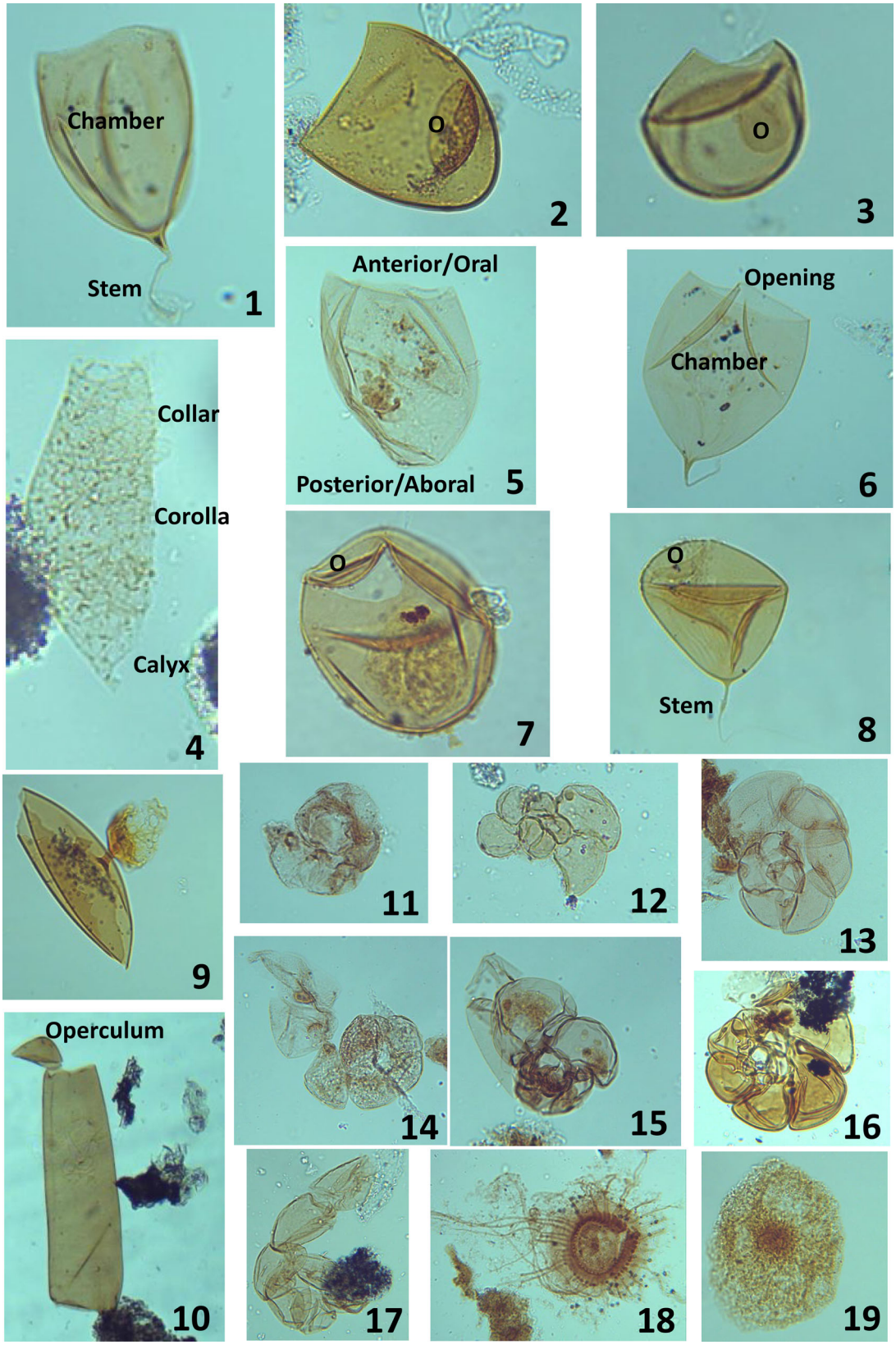

Plate 6. All photos ×400 unless otherwise mentioned. 1. Tintinnomorph type 1 with apiculate base with stalk; slide L3a; 9.2 × 160.3; size 71 × 55 μm; stem length 35 μm. 2. Tintinnomorph type 2 with rounded base; slide L5c; 20 × 152.2; size 77 × 71 μm; opening 60 μm. O: operculum. 3. Tintinnomorph type 3 spherical with small operculum; slide L3d; 6.8 × 149; size 42 × 40 μm. O: operculum. 4. Tintinnomorph type 4, elongated with ornamented wall; L5b; 9 × 148.2; size 78 × 29 μm (Lorica parts are labelled as shown in van Waveren 1994, figure 2). 5. Tintinnomorph type 5 with rounded base; slide L3b; 7 × 146; size 72 × 46 μm. 6. Tintinnomorph type 6 with apiculate base with stalk; slide L3a; 10.5 × 146.3; size 73 × 62 μm; stem length 19 μm. 7. Tintinnomorph type 7 spherical with small operculum; slide L3c; 7 × 141.5; size 310 μm (×100). O: operculum. 8. Tintinnomorph type 8 (striated capsule opening attached operculum); slide L3d; 5 × 131.6; size 51 × 49 μm; stem 18 μm. O: operculum. 9. Tintinnomorph type 9; slide L3d; 9 × 128.3; size 127 × 41 μm; appendage 51 × 34 μm. 10. Tintinnomorph type 10; L6c; 9 × 169; size 262 × 61 μm (×100). 11. Foraminiferal lining type 1; slide L3b; 7.5 × 134.5; size 64 μm. 12. Foraminiferal lining type 2; slide L6b; 4.5 × 157.2; size 61 μm. 13. Foraminiferal lining type 3; slide L3a; 6.5 × 143; size 104 × 74 μm. 14. Foraminiferal lining type 4; slide L3b; 5.5 × 157.5; size 105 × 66 μm. 15. Foraminiferal lining type 5; slide L3b; 13.5 × 156.5; size 73 × 51 μm. 16. Foraminiferal lining type 6; slide L4a; 7 × 164; size 95 × 77 μm. 17. Foraminiferal lining type 7; slide L4a; 21.5 × 144.5; size 114 × 70 μm. 18. Inderterminate form G (Fungal sporangium?); slide L2b; 17.5 × 151.5; size (D) 82 μm; process 30–150 μm (×100). 19. Oospore of *Oedogonium* (freshwater alga); slide L3c; 19.2 × 127; size 93 × 72 μm.

Microforaminiferal test linings occur as rare (1–4) to few (5–10) specimens in these samples. Al-Dubai et al. (2018) published on the diversity and distribution of benthic foraminifera in the Al-Kharrar Lagoon, eastern Red Sea coast of Saudi Arabia. They defined five assemblages characterising various environments in the lagoon, including a *Quinqueloculina seminula–Q. laevigata* intertidal assemblage, *Affinetrina quadrilateralis–Neorotalia calcar* and a few other forms. It is not possible to relate these benthic foraminifers to the microforaminiferal linings of the present study.

D2. Thecamoebians

Only two thecamoebian taxa were found in the present assemblages. Two specimens of *Geopyxella sylvicola* Bonnet & Thomas 1955 and a few more of *Centropyxis aculeata* Ehrenberg 1832 were observed (Tables 4 and 6). *Centropyxis aculeata* occurs in almost every lacustrine environment; however, it prefers warmer waters above the thermocline. Its morphology ranges from spiny to spineless. Limaye et al. (2017) reported the occurrence of *Geopyxella sylvicola*, a soil testate amoeba, from the tropical coastal lowlands of southwest India.

To the best of the author's knowledge, there are no published accounts of thecamoebian studies from the Arabian Peninsula. A report on the acid-resistant Cretaceous thecamoebian tests from the Arabian Peninsula (Kumar 2011) is the only publication on thecamoebian studies from this region. A useful illustrated key for the identification of Holocene lacustrine thecamoebian taxa (Kumar and Dalby 1998) is widely used for thecamoebian studies. Patterson and Kumar (2002) is a good review on testate rhizopod (Thecamoebian) research that discusses several aspects of studies on thecamoebians and their usefulness in palaeoenvironmental and (palaeo)limnological research.

D3. Tintinnids and worms

Tintinnids are complex eukaryotic protists and are part of the microzooplankton (size ranging between 20 and 200 μm) that inhabit primarily marine waters, but brackish and fresh waters as well (da Silva et al. 2017). They are heterotrophic organisms, feeding on photosynthetic algae and bacteria. Tintinnids produce a chitinous shell, also called a lorica; they have an oral opening at the anterior end. The posterior end of the lorica may be conical, globular or tubular. Most loricae are transparent and referred to as hyaline loricae. However, some tintinnids agglomerate mineral or biogenic particles to their lorica, hardening it. A hard bowl lorica is formed when the particles only stick to the posterior end (Agatha et al. 2013). The shape of the lorica is species specific; thus, species-level identification can be made based on only the lorica. However, there are considerable intraspecific morphological variations related to the life-cycle stages of the ciliate (Agatha et al. 2013).van Waveren (1994) introduced the term 'tintinnomorphs' to emphasise that palynomorphs resembling tintinnids cannot always be separated into loricae or cysts and may even represent cysts of other protozoans. da Silva et al. (2017) expanded the concept of 'tintinnomorphs' to encompass the group of palynomorphs resembling organic remains of tintinnids, which are not always identifiable as true loricae, cysts or pouches corresponding to other protozoans, and may even represent other structures of distinct organisms, such as rotifers and turbellarians. Many loricae and cysts occur in palynological preparations, especially in modern marine and marginal marine sediments (see references in da Silva et al. 2017) and are classified as zoomorphs (Traverse 1994).

van Waveren (1994) described, illustrated and categorised tintinnomorphs in an informal morphological system. Tintinnomorphs are organic remains that include loricae, cysts and the stalked pouches in which cysts were originally encapsulated. Both loricae and cysts are considered to display wide morphological varibility. Tintinnomorphs resemble organic remains of tintinnids, but are not necessarily identifiable as true lorica, cysts or pouch. In this study, 17 tintinnomorphs are described using the terminology of van Waveren (1994), as follows.

Tintinnomorph type 1 (Plate 6, figure 1).

Description: Greyish yellow, egg shaped – orally blunt, with short triangular calyx and a long thread-like stem, wall smooth, opening large, between 0° and 30°, no collar.

Size: 71 × 55 μm; stem length 35 μm.

Comments: Tintinnomorph type 1 corresponds to the ESOBNO (egg shaped orally blunt with unornamented wall) type of van Waveren (1994, figure 3/4).

Tintinnomorph type 2 (Plate 6, figure 2).

Description: Yellow, elliptical, no calyx and no stem, wall smooth, opening large, between 0° and 30°, no collar. Operculum lies inside the chamber.

Size: 77 × 71 μm; opening 60 μm.

Comments: Tintinnomorph type 2 corresponds to the ELLIPNO (elliptical shape with unornamented wall) type of van Waveren (1994, figure 3/1).

Tintinnomorph type 3 (Plate 6, figure 3).

Description: Brownish, spherical, no calyx and no stem, wall smooth, opening small, more than 75°, no collar. Operculum lies inside the chamber.

Size: 42 × 40 μm.

Comments: Tintinnomorph type 3 corresponds to the SPHERNO (spherical shape with unornamented wall) type of van Waveren (1994, figure 3/0).

Tintinnomorph type 4 (Plate 6, figure 4).

Description: Translucent, elongated-elliptical, calyx short, triangular but no stem, wall ornamented, opening medium, 30°–75°, short collar.

Size: 78 × 29 μm.

Comments: Tintinnomorph type 4 corresponds to the ELELNO (elongated elliptical shape with unornamented wall) type of van Waveren (1994, figure 3/2).

Tintinnomorph type 5 (Plate 6, figure 5).

Description: Light brown, elliptical, no calyx and no stem,

wall finely ornamented, opening medium, 30–75°, no collar. This form resembles Tintinnomorph type 2 but its opening is medium and there is no operculum inside the chamber.

Size: 72 × 46 μm.

Comments: Tintinnomorph type 5 corresponds to the ELLIPNO-1 type of van Waveren (1994, figure 3/1).

Tintinnomorph type 6 (Plate 6, figure 6).

Description: Light brown, egg shaped – orally blunt, with no calyx and a long thread-like stem, wall smooth, opening large, between 0° and 30°, no collar.

Size: 73 × 62 μm; stem length 19 μm.

Comments: Tintinnomorph type 6 corresponds to the ESOBNO type of van Waveren (1994, figure 3/4).

Tintinnomorph type 7 (Plate 6, figure 7).

Description: Yellow, very large, spherical, no calyx and no stem, wall smooth, opening small, more than 75°, no collar. Operculum lies on the mouth but does not completely cover it.

Size: 310 μm.

Comments: Tintinnomorph type 7 corresponds to the SPHERNO type of van Waveren (1994, figure 3/0).

Tintinnomorph type 8 (Plate 6, figure 8).

Description: Yellow, approximately triangular, no calyx but long thread-like stem, wall ornamented, wrinkled, wrinkles run parallel to the edge of lorica, opening small, more than 75°, no collar. Operculum attached to the mouth but does not completely cover it.

Size: 51 × 49 μm; stem 18 μm.

Comments: Tintinnomorph type 8 corresponds to the TRIANO-1 (triangular shape with unornamented wall) type of van Waveren (1994, figure 3/9).

Tintinnomorph type 9 (Plate 6, figure 9).

Description: Yellow, elliptical, no calyx and no stem, wall smooth, opening not clear due to folding in the wall, no collar. There is an appendage on the wall.

Size: 127 × 41 μm; appendage 51 × 34 μm.

Comments: Tintinnomorph type 9 approximately corresponds to the ELLIP type of van Waveren (1994, figure 3/1). The appendage is unique to this form and has not been reported in the literature.

Tintinnomorph type 10 (Plate 6, figure 10).

Description: Large, greyish yellow, rectangular, no calyx and no stem, wall smooth, opening small, more than 75°, no collar. Operculum lies close to the mouth but does not cover it.

Size: 262 × 61 μm.

Comments: Tintinnomorph type 10 corresponds to the RECTNO-1 (rectangular shape with unornamented wall) type of van Waveren (1994, figure 3/6).

Tintinnomorph type 11 (Plate 4, figure 5).

Description: Almost translucent, egg shaped – aborally blunt, no calyx and no stem, wall agglutinated with sand particles around corolla and diatoms around collar, opening large, 0–30°.

Size: 88 × 51 μm; opening 31 μm.

Comments: Tintinnomorph type 11 corresponds to the ESABO-1 type of van Waveren (1994, figure 3/3).

Tintinnomorph type 12 (Plate 5, figure 6).

Description: Grey, egg shaped – aborally blunt, no calyx and no stem, wall ornamented with spinules around corolla, opening medium, 30–75°, with narrow parallel collar.

Size: 95 × 42 μm; spinules 8–10 μm.

Comments: Tintinnomorph type 12 corresponds to the ESABO-2 type of van Waveren (1994, figure 3/3).

Tintinnomorph type 13 (Plate 4, figure 12).

Description: Grey, rectangular, no calyx and no stem, wall agglutinated with sand particles around corolla, opening small, more than 75°, with short converging, annulate collar.

Size: 68 × 43 μm; opening 16 μm.

Comments: Tintinnomorph type 13 corresponds to the RECTO (rectangular shape with ornamented wall) type of van Waveren (1994, figure 3/6).

Tintinnomorph type 14 (Plate 4, figure 16).

Description: Grey, egg shaped – orally blunt, short, triangular calyx and no stem, wall agglutinated with sand particles around corolla, opening medium, 30–75°, with no collar.

Size: 86 × 68 μm.

Comments: Tintinnomorph type 14 corresponds to the ESOBO-1 type of van Waveren (1994, figure 3/4).

Tintinnomorph type 15 (Plate 4, figure 19).

Description: Yellow, triangular, with short triangular calyx and no stem, wall ornamented with fine reticulation, opening more than 75°, no collar.

Size: 60 × 59 μm.

Comments: Tintinnomorph type 15 corresponds to the TRIA (triangular shape) type of van Waveren (1994, figure 3/9).

Tintinnomorph type 16 (Plate 4, figure 18).

Description: Grey, elliptical, no calyx and no stem, wall agglutinated with sand particles around corolla, opening small, more than 75°, with short diverging collar.

Size: 62 × 47 μm; opening 18 μm.

Comments: Tintinnomorph type 16 corresponds to the ELLIPO (elliptical shape with ornamented wall) type of van Waveren (1994, figure 3/1).

Tintinnomorph type 17 (Plate 5, figure 15).

Description: Greyish yellow, egg shaped – aborally blunt, no calyx and no stem, wall smooth and partly folded, opening medium, 30–75°, with no collar.

Size: 76 × 59 μm.

Comments: Tintinnomorph type 17 corresponds to the ESABNO-1 (egg shaped, aborally blunt with unornamented wall) type of van Waveren (1994, figure 3/3).

The orientation and morphological features of the tintinnomorphs are shown in Plate 6. Their nomenclature is based on van Waveren (1994); the main morphological features of a lorica are: corolla enclosing a chamber; opening (sometimes with operculum); calyx (a hollow appendix); stem (a massive appendix); horn (calyx plus stem); and collar. The side with the opening

Table 1. Distribution of pollen and spores.

	SAMPLES						
Angiosperm pollen	L1	L2	L3	L4	L5	L6	L7
***Acacia* sp.**	2	1				1	
***Artemisia* sp.**				1			
cf. *Avicennia marina*						1	
cf. *Casuarina* sp.		1					
***Calligonum* sp.**		1					
Chenopodiaceae/Amaranthaceae			2			6	
Cyperaceae	3	1	1		1		
***Euphorbia* sp.**			1			1	
***Neocouperipollis* sp.**	1	2				2	
***Palmaepollenites* sp.**	1	2	3				
***Palmidites* sp.**	1		2		1		
***Potomogeton* sp.**	1		2				
Rhizophora mucronata					1		
***Nypa* sp.**		1	2				
***Trichotomosulcites* sp.**						1	
Tricolpate psilate			1				
Tricolpate scabrate			1			1	1
***Verrualetes* sp.**							1
Gymnosperm pollen							
***Juniperus* pollen**						1	
***Pinus* sp.**			2				
***Podocarpus* sp.**			1			1	
Spores							
***Laevigatosporites* sp.**						1	
***Lycopodiumsporites* sp.**						1	
***Polypodiisporites* sp.**						2	
***Triplanosporites* sp.**						1	
***Verrucosisporites* sp.**						1	

Table 2. Distribution of dinoflagellate cysts and other algal remains.

	SAMPLES						
Dinoflagellate cysts	L1	L2	L3	L4	L5	L6	L7
?*Operculodinium* sp.					1		
***Peridinium* sp.**		1					
Spiny round brown cyst		1					
Dinoflagellate cyst type A	1						
Dinoflagellate cyst type B	1						
Dinoflagellate cyst type C	1						
Dinoflagellate cyst type D		1					
Dinoflagellate cyst type E			1				
Dinoflagellate cyst type F						1	
Algal remains							
Algal body (unidentified)	1	1		1			
Algal cells type A		1	3		1		
Algal cells type B		1	1		1		
Algal cyst (unidentified)		1	1		2	3	
***Botryococcus* sp.**	1						
Colonial alga/Cyanobacteria	2						
***Concentricystis* sp.**						3	
***Gleotrichia* sp.**		1					
***Lecaniella* sp.**		1			1	1	
***Rivularia* sp.**						1	
***Spirogyra* zygospore**					1		

is termed the oral side, and the opposite is the aboral side. The distribution of tintinnomorphs is presented in Tables 4 and 6.

There is a possibility that tintinnomorphs described here might be Neorhabdocoela oocytes as described by Haas (1996), because there is certain morphological resemblance between them. However, the author prefers to classify them as tintinnomorphs because van Waveren (1994) provided detailed descriptive and illustrated terminology in her informal morphological system. Tintinnomorphs, as stated earlier, is a collective term for loricae, cysts and stalked pouches of tintinnids, and some of them morphologically resemble oocytes (egg capsules) of aquatic flatworms of the order Neorhabdocoela (e.g.

Table 3. Distribution of fungal spores, hyphae and fruit bodies.

	SAMPLES						
Fungal remains	L1	L2	L3	L4	L5	L6	L7
Biporipsilonites maximus						1	
Brachysporisporites sp.		1	1		1		
Callimothallus type fruit body	4	2	2				
Dicellaesporites sp.			1				
Dictyosporites sp.	6		2				
Diporicellaesporites sp.	1						
Glomus sp.						2	
Inapertisporites sp.				1		2	1
Monoporisporites sp.			2		1		
Multicellites sp.						1	
Phragmothyrites sp.				1			
Trichothyrites sp.				1			
Fungal hyphae		4		1	1		
Fungal sporangium		2		1			
Unidentified fungal spores	2	1	4	1	4		
Unidentified fungal remains	1		2	1	1	1	

Haas 1996, plate 1-g). Neorhabdocoela oocytes are typically elliptical to spherical and dark brown in colour, and relatively large in size (60–600 μm), whereas tintinnomorphs, in contrast, are usually cup shaped, oval or of diverse shapes, pale yellow and relatively smaller in size. Neorhabdocoela oocytes occur predominantly in freshwater environments, while the present assemblage is from an intertidal environment.

A high morphological diversity of tintinnomorphs indicates a high diversity of tintinnids in the southern Red Sea zooplankton; however, their presence is usually numerically rare in the intertidal sediments. Abou Zaid and Hellal (2012) published an assemblage of modern tintinnids from the Hurghada coast of the Red Sea in Egypt. However, it is difficult to assign a species or genus name to the titinnomorphs based only on the shape of lorica or cyst.

D4. Crustacean and annelid palynomorphs

The crustacean and annelid remains found in these palynomorph assemblages are diverse and occur in all samples, although their absolute numbers range from rare to few. A total of 17 forms, including 12 crustacean and seven annelid forms, occur in these samples (Tables 5 and 6). A neoichnological study reported several biogenic traces that occur in the intertidal and supratidal flats of the same locality as the present study (Kumar 2017). The biogenic traces were interpreted to have been formed by gastropods, land hermit crabs *Coenobita clypeatus*, ghost crab *Ocypode quadrata*, insects, beetles, sand wasps, and *Arenicola marina*, a large marine worm of the phylum Annelida; it is also known as lugworm or sandworm (Kumar 2017). Copepods (subphylum Crustacea; subclass Copepoda) inhabit the area of the present study as well. They are microcrustaceans (0.5–2 mm in size) that normally occur in nearly every freshwater and saltwater habitat as planktic or benthic organisms. They have two pairs of antennae and a single red compound eye; they are mostly crawlers, walkers, and burrowers in terrestrial environments, but live wherever water is generally available (Gleime 2017).

It is logical to suggest that the chitinous remains of crustaceans and annelids observed in this study most likely belong to these invertebrate animals. At present it is not

Table 4. Distribution of microforaminifera, thecamoebians and tintinnomorphs.

	SAMPLES						
Microforaminifera	L1	L2	L3	L4	L5	L6	L7
Microforaminiferal test linings type 1			1				
Microforaminiferal test linings type 2						1	
Microforaminiferal test linings type 3			1				
Microforaminiferal test linings type 4			1				
Microforaminiferal test linings type 5			1				
Microforaminiferal test linings type 6				1	1		
Microforaminiferal test linings type 7				1			
Thecamoebians							
Centropyxis aculeata	1	2			2		
Geopyxella sylvicola		1					
Tintinnomorphs							
Tintinnomorph type 1			2	1			1
Tintinnomorph type 2				1	1	1	
Tintinnomorph type 3			2	1	2		
Tintinnomorph type 4			1		1		
Tintinnomorph type 5			1				
Tintinnomorph type 6			3	2	1	1	
Tintinnomorph type 7			2				
Tintinnomorph type 8			1			1	
Tintinnomorph type 9			1				
Tintinnomorph type 10					1	1	
Tintinnomorph type 11	1		1				
Tintinnomorph type 12	1						
Tintinnomorph type 13	1						
Tintinnomorph type 14		1					
Tintinnomorph type 15		1	1	2	1	1	
Tintinnomorph type 16		1			1		
Tintinnomorph type 17			1	1			

always possible to relate such palynomorphs to their parent organisms. More work needs to be done on this matter.

E. Miscellaneous and indeterminate palynomorphs

E1. Miscellaneous palynomorphs

Miscellaneous palynomorphs include stomata; leaf epidermis showing stomata; charcoal; and phytoliths. All these palynomorphs are rare or few in occurrence and do not occur in all samples (Table 6). Leaf epidermis, probably of grass, with stomata as well as phytoliths indicate the presence of the family Poaceae in the region, but no Poaceae pollen was observed in these assemblages. The presence of charcoal indicates natural forest fires or possibly wood burning due to human activity.

E2. Indeterminate palynomorphs

A total of seven indeterminate forms were identified and designated A through G. Most of these indeterminate palynomorphs occur rarely in the samples (Table 6). Tentative suggestions of their affinities are as follows: indeterminate form A may be worm oocytes with operculum; indeterminate form B may be an algal spore; indeterminate form C may be Cyanobacteria; indeterminate form D may be *Pseudoschizaea/Concentricystis* sp.?; indeterminate form E may be a crustacean egg; indeterminate form F may be an algal cyst; and indeterminate form G may be a fungal sporangium.

Distribution of palynomorphs

The distribution of palynomorphs in these samples is reported in Tables 1–6. Palynomorph assemblages were

Table 5. Distribution of crustacean and annelid palynomorphs.

	SAMPLES						
Crustacean palynomorphs	L1	L2	L3	L4	L5	L6	L7
Crustacean thoracic segment		1					
Crustacean appendage	1						
Crustacean head (?)					1	3	
Crustacean head					2	2	
Ostracod jaw			2		1	1	
Scolecodont					2	2	
Insect wing						1	
Insect exoskeleton			1		1	3	1
Crustacean appendage			1			1	
Crustacean antenna (?)		2				1	
Copepod fragment					1	1	
Copepod antenna						2	
Annelid palynomrphs							
Small turbellarian worm			1		2	2	
Annelid palynomorph	1		1			3	
Annelid jaw					1	1	
Worm						2	1
Annelid remains (?)						1	1

Table 6. Distribution of palynomorphs and palynomorph groups.

TAXA	SAMPLES						
	L1	L2	L3	L4	L5	L6	L7
Pollen and spores							
Angiospermous pollen	F	F	C	R	R	C	R
Gymnospermous pollen	R		R				
spores						F	
Algal remains							
Botryococcus sp.	R	R	R				
Algal remains (indet.)	C	C	F	F	C	F	
Cyanobacteria	R					R	
Dinoflagellate cysts	R	R	R		R	R	
Concentricystis sp.		R				R	
Lecaniella sp.		R				R	R
Oospore of Oedogonium			R		R		
Tetraporina sp.					R		
Fungal remains							
Glomus sp.	R		C	R		F	
Spores + hyphae	C	R	C	F		F	R
Fruit bodies	A	F	VC	F	F	R	
Indeterminate forms	F	C	VC	F	C	C	R
Protists and invertebrates							
Copepod eggs	R	VC	VC	C	C	C	R
Tintinnomorphs	C	C	A	VC	VC	F	R
Scolecodonts			R		F	F	R
Microforaminifera		R	R	F		R	R
Crustacean palynomorphs	R	F	C	C	C	A	F
Annelid palynomorphs	C	VC	VC	R	R	C	R
Thecamoebians	R	R					
Indeterminate palynomorphs							
Crustacean antennae ?	A	A	C	A	A	VC	VC
Indeterminate Palynomorph A	R	R					
Indeterminate Palynomorph B	R	R					
Indeterminate Palynomorph C	F	R					
Indeterminate Palynomorph D					R		
Indeterminate Palynomorph E						R	
Indeterminate Palynomorph F		R					
Indeterminate Palynomorph G		R					
Phytoliths						F	
Charcoal	R	R	R	R	R	R	R

Rare (R): 1-4 specimens; Few (F): 5-10 specimens; Common (C): 11-25 specimens; Very Common (VC): 26-50 specimens; Abundant (A): 51 or more specimens.

divided into groups of fossils – pollen and spores (Table 1); dinoflagellate cysts and other algal remains (Table 2); fungal spores, hyphae and fruit bodies (Table 3); microforaminifera, thecamoebians and tintinnomorphs (Table 4); crustacean and annelid palynomorphs (Table 5) – and the distribution of palynomorphs and palynomorph groups is given in Table 6.

Sample L1 has abundant biodegraded terrestrial organic matter (OM) that includes various types of cuticles, trachieds, fungal hyphae, spores, algal filaments, dispersed unidentifiable forms and rare fragments of charcoal. The assemblage contains many microscopic remains of protists and invertebrates. A tentatively identified form of crustacean antennae is abundant in this sample. Pollen and spores, and algal and fungal remains, are represented by only rare to few specimens. The palynomorph composition in samples L2 and L3 is very similar to that of sample L1. The assemblage of this sample is dominated by protists such as tintinnomorphs, and invertebrates such as crustacean and annelid palynomorphs. Rare specimens of microforaminiferal linings and a few unidentified forms occur in this sample as well. The palynomorph assemblages of samples L4, L5 and L6 include very little biodegraded terrestrial OM, few cuticles, trachieds, rare fungal hyphae, spores, rare dispersed unidentifiable forms, and rare fragments of charcoal. The predominant palynomorphs in all these samples are derived protists and invertebrates. Crustacean antennae (?) are either abundant or very common in these samples. Sample L7 is almost barren; it contains very little biodegraded terrestrial OM, few cuticles, trachieds, fungal remains, and rare fragments of charcoal.

Conclusions

1. Seven samples, including four from semi-consolidated surface sediments of the tidal flats, two from a small pond on the tidal flats and one from a subtidal environment along the southern Red Sea coast – were studied.
2. Four clay to fine sand samples (L1 through L4) are from tidal flats, two clay samples (L6 and L7) are from a small pond with abundant algae and sample L5 is from subtidal mud at 1.5 m water depth.
3. These samples yielded low numbers but a high diversity of palynomorphs (Tables 1–6) and are illustrated in Plates 1–6 to show their taxonomic diversity.
4. These palynomorphs exhibit diverse affinities and their sources are outlined. They have been divided into five groups: (A) pollen and spores; (B) dinoflagellate cysts and algal remains; (C) fungal spores, hyphae and fruit bodies; (D) protists and invertebrate remains; and (E) miscellaneous and unidentified forms.
5. The protists and invertebrate remains represent a large and diverse group that includes microforaminiferal linings, thecamoebians, tintinnomorphs, and crustacean and annelid palynomorphs.
6. Palynomorphs of these assemblages belong to both marine and terrestrial environments and are of autochthonous and allochthonous origins.
7. An attempt has been made to identify each palynomorph and relate it to its parent organism, plant or animal, and discuss its environment.
8. This is the first such study in and around the Arabian Peninsula.

Acknowledgements

I thank my former colleagues from King Fahad University of Petroleum and Minerals (KFUPM), Saudi Arabia: Lamidi Babalola, Michael Kaminski and Khalid Ramadan. They helped during the field trip and sample collection. Asif Khan prepared the location map, and Osman Abdullatif and all of us discussed various aspects of this project. I thank KFUPM for financial support of the field trip. I am thankful to Dr Peta Mudie (Geological Survey of Canada) and Dr Francine McCarthy (Brock University) for helping me in identifying certain palynomorphs. I dedicate this paper to my dear friend Sunil Kumar, former director Geological Survey of India, Lucknow, India. I also thank my son, Anshuman Kumar, for linguistic improvements to this research paper.

Disclosure statement

No potential conflict of interest was reported by the author.

Notes on contributor

ARUN KUMAR did M.Sc. (Geology) from Lucknow University, India, Ph.D. (Stratigraphic Palynology) from Michigan State University, USA, and a second Ph.D. (Environmental Micropaleontology) from Carleton University, Canada, and worked as a post-doctoral research fellow at Sheffield University, UK, Nagasaki University, Japan and Carleton University, Canada. He taught various courses in Geology at Kumaun University, India, University of the West Indies, Jamaica, and King Fahad University of Petroleum and Minerals (KFUPM), Saudi Arabia. He also worked with the petroleum industry as a palynologist and biostratigrapher with the Oil and Natural Gas Corporation, India, P.T. Corelab Indonesia, KFUPM, and Sirte Oil Company, Libya. During all these assignments he worked on several projects on Permian, Jurassic, Cretaceous and Tertiary biostratigraphy, and basin exploration. In addition to palynology, his other research interests include application of thecamoebians as proxies for Quaternary climate and environmental changes, and study of Holocene dinoflagellate cysts and benthic foraminifera in the fjords of Vancouver Island, Canada. He has studied mangroves surrounding the Arabian Peninsula, and his new research interest is in natural hazards. He has published extensively on these subjects, and along with a colleague, edited a volume on Paleotsunami (Natural Hazards, 2012, 63-1). At present he is a Research Associate in the Department of Earth Science, Carleton University, Ottawa, Canada.

References

Abou Zaid MM, Hellal AM. 2012. Tintinnids (Protozoa: Ciliata) from the coast of Hurghada Red Sea. The Egyptian Journal of Aquatic Research. 38(4):249–268.

Agatha S, Laval-Peuto M, Simon P, et al. 2013. The *Tintinnid lorica*. In: Dolan JR, editors. The biology and ecology of tintinnid ciliates: models for marine plankton. New York: John Wiley & Sons; p. 42–84.

Al-Ameri TK, Jassim SY. 2009. Environmental changes in the wetlands of southern Iraq based on palynological studies. Arabian Journal of Geoscience. 4:443–461.

Al-Dabbas MA, Abba MA, Al-Khafaji RM. 2010. Dust storm loads analyses: Iraq. Arabian Journal of Geoscience. 5:121–131.

Al-Dubai TA, Abu-Zied RH, Basaham AS. 2018. Diversity and distribution of benthic foraminifera in the Al-Kharrar Lagoon, eastern Red Sea coast, Saudi Arabia. Micropaleontology. 63(5):275–303.

Anderson RS, Homola RA, Davis RB, Jacobson GL. Jr. 1984. Fossil remains of the mycorrhizal fungal *Glomus fasciculatum* complex in post glacial lake sediments from Marine. Canadian Journal of Botany. 62(11): 2325–2328.

Awadh SM, Ali Mo, Ali RA. 2010. Mineralogy and palynology of the Mesopotamian plain sediments, Central Iraq. Arabian Journal of Geoscience. 4:1261–1271.

Berggren WA. 1969. Micropaleontologic investigations of Red Sea cores: summation and synthesis of results. In: Degens ET, Ross DA, editors. Hot brines and recent heavy metal deposits in the Red Sea. New York: Springer-Verlag; p. 329–335.

Bradford MR. 1975. New dinoflagellate cyst genera from the recent sediments of the Persian Gulf. Canadian Journal of Botany. 53(24): 3064–3074.

Bradford MR, Wall DA. 1984. The distribution of recent organic-walled dinoflagellate cysts in the Persian Gulf, Gulf of Oman, and northwestern Arabian Sea. Palaeontographica, Abteilung B. 192:16–84, pl. 1–6.

Cole JB. 1992. Fresh water dinoflagellate cysts and acritarchs from Neogene and Oligocene sediments of the South China Sea and adjacent areas. In: Head MJ, Wrenn JH, editors. Neogene and quaternary dinoflagellate cysts and acritarchs. Dallas: American Association of Stratigraphic Palynologists Foundation; p. 181–196.

Cook EJ. 2009. A record of late quaternary environments at lunette-lakes Bolac and Turangmoroke, Western Victoria, Australia, based on pollen and a range of non-pollen palynomorphs. Review of Palaeobotany and Palynology. 153(3–4):185–224.

Cook EJ, van Geel B, van der Kaars S, van Arkel J. 2011. A review of the use of non-pollen palynomorphs in palaeoecology with examples from Australia. Palynology. 35 (2):155–178.

da Silva WG, de Souza PA, van Waveren I. 2017. New Insights on the systematic classification of certain palynological taxa (tintinnomorphs) from Holocene deposits of the Coastal Plain of Southern Brazil. Revista Brasileira de Paleontologia. 20(3):321–332.

de Vernal A. 2009. Marine palynology and its use for studying nearshore environments. Deep-sea to coastal zones: methods and techniques for studying paleoenvironments. IOP Conference Series: Earth and Environmental Science. 5 (2009):012002.

El-Naggar SM, El-Husseini N. 2001. Pollen Atlas of the Flora of Egypt. 2. Species of Polygonaceae. Taeckholmia. 21(1):143–151.

Elshanawany R, Zonneveld K, Ibrahim MI, Kholeif S. 2010. Distribution patterns of recent organic-walled dinoflagellate cysts in relation to environmental parameters in the Mediterranean Sea. Palynology. 34(2):233–260.

Elsik WC. 1996. Fungi. Chapter 10. In: Jansonius J, McGregor DC, editors. Palynology: principles and applications, vol. 1. Salt Lake City (UT): American Association of Stratigraphic Palynologists Foundation, Publishers Press; p. 293–306.

Gelorini V, Ssemmanda I, Verschuren D. 2012. Validation of non-pollen palynomorphs as paleoenvironmental indicators in tropical Africa: Contrasting ~200-year paleolimnological records of climate change and human impact. Review of Palaeobotany and Palynology.. 186: 90–101.

Gleime JM, 2017. Arthropods: Crustacea: Copepoda and Cladocera. Chapter 10-1. In: Glime JM, editor. Bryophyte ecology Volume 2. Bryological interaction. E book sponsored by Michigan Technological University and the International Association of Bryologists. Houghton (MI): Michigan Technological University. Available from: http://digitalcommons.mtu.edu/bryophyte-ecology2.

Grainger D. 2007. The geological evolution of Saudi Arabia. A voyage through space and time. Jeddah (Saudi Arabia): Saudi Geological Survey; p. 262.

Haas JN. 1996. Neorhabdocoela oocytes: palaeoecological indicators found in pollen preparations from Holocene freshwater lake sediments. Review of Palaeobotany and Palynology. 91(1–4):371–382.

Hanauer E. 1988. The Egyptian Red Sea: a diver's guide. San Diego (CA): Aqua Quest Publications, Inc.

Head MJ. 1993. Dinoflagellates, sporomorphs, and other palynomorphs from the Upper Piocene St. Earth Beds of Cornwall, southwestern England. Journal of Paleontology. 67(S31):1–62, Part III of III.

Jado AR, Hotzl H, Roscher B. 1990. Development of sedimentation along the Saudi Arabian Red Sea coast. Journal of King Abdul Aziz University. 3(1):47–62.

Jado AR, Zölt JG. 1984. Quaternary Paeriod in Saudi Arabia. Vol. 2. Vienna: Springer-Verlag; p. 360.

Kalgutkar RM, Jansonius J. 2000. Synopsis of fossil fungal spores, mycelia and fructifications. AASP contribution series no. 39. Dallas (TX): American Association of Stratigraphic Foundation Series; 423p.

Khan MA, Kumar A, Muqtadir A. 2010. Distribution of mangroves along the Red Sea coast of the Arabian Peninsula: Part-2: the southern coast of western Saudi Arabia. e-Journal Earth Science India. 3 (3):154–162.

Kholeif S. 2004. Palynology and paleovegetation reconstruction in late Quaternary sediments in the southern Suez Isthmus. Journal of African Earth Sciences . 40(1–2):31–112.

Kholeif S. 2007. Palynology of mangrove sediments in the Hamata Area, Red Sea coast, Egypt: vegetation and restoration overview. In: Isermann M, Keihl K, editors. Restoration of coastal ecosystems. Coastline reports, vol. 7. Leiden (Netherlands): EUCC; p. 5–16. Available from: https://eucc-d-inline.databases.eucc-d.de/files/documents/00000331_Artikel%202_Kholeif.pdf.

Kholeif SEA, Mudie PJ. 2009. Palynological records of climate and oceanic conditions in the late Pleistocene and Holocene of the Nile Cone, southeastern Mediterranean. Palynology. 33(1):1–24.

Krueger AM, McCarthy F. 2016. Great Canadian Lagerstätten 5. Crawford Lake: a Canadian Holocene Lacustrine Konservat-Lagerstätte with two-century-old viable dinoflagellate cysts. Geoscience Canada. 43(2): 123–132.

Kumar A. 2011. Acid-resistant Cretaceous thecamoebian tests from the Arabian Peninsula: a suggestion for study of agglutinated rhizipods in palynological slides. Journal of Micropalaeontology. 30(1):1–5.

Kumar A. 2013. Invited Paper: natural hazards of the Arabian Peninsula; their causes and possible remediation. In: Sinha, R, Ravindra, R, editors. Earth system processes and disaster management, society of earth scientists series 1. Berlin: Springer-Verlag; p. 155–180.

Kumar A. 2017. Recent biogenic traces from the coastal environments of the southern Red Sea coast of Saudi Arabia. Arabian Journal of Geosciences. 10 (22):3–11..

Kumar A, Dalby AP. 1998. Identification key for Holocene lacustrine arcellacean (thecamoebian) taxa. Palaeontologia Electronica. 1(1):1–39.

Kumar A, Khan MA, Muqtadir A. 2010. Distribution of mangroves along the Red Sea coast of the Arabian Peninsula: Part-1: the northern coast of western Saudi Arabia. e. Journal Earth Science India. 3 (1):28–42.

Kumar A, Khan MA, Muqtadir A. 2011. Distribution of mangroves along the Red Sea coast of the Arabian Peninsula: Part-3: the coast of Yemen. e-Journal Earth Science India. 4 (II):29–38.

Kumaran KPN, Limaye RB, Nair KM, Padamlal D. 2008. Palaeoecological and palaeoclimate potential of subsurface palynological data from the Late Quaternary sediments of South Kerala Sedimentary Basin, southwest India. Current Science. 95(4):515–526.

Limaye RB, Kumaran KPN, Nair KM, Padamlal D. 2007. Non-pollen palynomorphs as potential palaeoenvironmental indicators in the Late Quaternary sediments of the southwest coast of India. Current Science. 92(10):1370–1382.

Limaye RB, Padmalal D, Kumaran K. 2017. Cyanobacteria and testate amoeba as potential proxies for Holocene hydrological changes and climate variability: evidence from tropical coastal lowlands of SW India. Quaternary International. 443:99–114.

Mathison SW, Chmura GL. 1995. Utility of microforaminiferal test lining in palynological preparations. Palynology. 19(1):77–84.

Matsuoka K, Yurimoto T, Chong VC, Man A. 2017. Marine palynomorphs dominated by heterotrophic organism remains in the tropical coastal shallow-water sediment; the case of Selangor Coast and the estuary of the Manjung River in Malaysia. Paleontological Research. 21(1): 14–26.

McCarthy FMG, Mertens KN, Ellegaard M, Sherman K, Pospelova V, Ribeiro S, Blasco S, Vercauteren D. 2011. Resting cysts of freshwater dinoflagellates in southeastern Georgian Bay (Lake Huron) as proxies of cultural eutrophication. Review of Palaeobotany and Palynology. 166(1–2):46–62..

McCarthy FMG, Riddick NL, Volik O, Danesh DC, Krueger AM. 2018. Algal palynomorphs as proxies of human impact on freshwater resources in the Great Lakes region. Anthropocene. 21:16–31.

Medeanic S, Zamora N, Correa I. 2008. Non-pollen palynomorphs as environmental indicators in the surface samples from mangrove in Costa Rica. Revista Geologica de America Central. 39:27–51.

Mertens KN, Rengefors K, Moestrup Ø, Ellegaard M. 2012. A review of recent freshwater dinoflagellate cysts: taxonomy, phylogeny, ecology and palaeocology. Phycologia. 51(6):612–619.
Migahid AM. 1978. Flora of Saudi Arabia. 2 Vols, 2nd ed. Riyadh: Riyadh University Publications; p. 650.
Monga P, Kumar M, Joshi Y. 2015. Morphological variations and depositional processes of microforaminiferal linings in the early Tertiary sediments of northeastern and northwestern India. The Palaeobotanist. 64(2):129–138.
Montoya E, Rull V, van Geel B. 2010. Non-pollen palynomorphs from surface sediments along an altitudinal transect of the Venezuelan Andes. Palaeogeography, Palaeoclimatology, Palaeoecology. 297(1):169–183.
Mudie PJ, Leroy SAG, Marret F, Gerasimenko N, Kholeif SEA, Sapelko T, Filipova-Marinova M. 2011. Non-pollen palynomorphs: Indicators of salinity and environmental change in the Caspian-Black Sea-Mediterranean corridor. The Geological Society of America Special Paper. 473:1–27.
Mudie PJ, Marret F, Rochon R, Aksu AE. 2010. Non-pollen palynomorphs in the Black Sea corridor. Vegetation History and Archaeobotany. 19(5–6):531–544.
Mudie JP, Yanko-Holmbach V. 2019. Microforaminiferal linings as proxies for paleosalinity and pollution: Danube Delta example. Micropaleontology. 65 (1):1–19.
Patterson RT, Kumar A. 2002. A review of current testate rhizopod (Thecamoebian) research in Canada. Paleogeography, Paleoecology, Paleoclimatology. 180(1–3):225–251.
Rasul NMA, Stewart I. 2015. The Red Sea: the formation, morphology, oceanography and environment of a young ocean basin. Berlin: Springer Earth System Sciences; 620p.
Saifullah SM. 1996. Mangrove ecosystem of Saudi Arabian Red Sea coast – an overview. Journal of King Abdulaziz University-Marine Sciences. 7(1):263–270.
Shamso EM, Toshiyuki F. 2012. The pollen flora of Faiyum. Taeckholmia. 32(1):1–70.
Stancliffe R. 1996. Microforaminiferal linings. In: Jansonius J, McGregor DC, editors, Palynology: principles and applications, vol. 1. Dallas (TX): American Association of Stratigraphic Palynologists Foundation; p. 373–379.
Thomas J. 2011. Plant Diversity in Saudi Arabia. Riyadh (Saudi Arabia): Herbarium, Department of Botany and Microbiology, King Saud University. http://plantdiversityofsaudiarabia.info/index.htm. Last accessed on September 10, 2019.
Traverse A. 1994. Sedimentation of palynomorphs and palynodebris: an introduction. In: Traverse A, editor. Sedimentation of organic particles. Cambridge (MA): Cambridge University Press; p. 1–8.
van Geel B. 1972. Palynology of a section from the raised peat bog "Wietmarscher Moor" with special reference to fungal remains. Acta Botanica Neerlandica. 21(3):261–284.
van Geel B. 1976. Fossil spores of Zygnemataceae in ditches of a pre-historic settlement in Hoogkarspel (The Netherlands). Review of Palaeobotany and Palynology. 22(4):337–344.
van Geel B. 1986. Application of fungal and algal remains and other microfossils in palynological analyses. In: Bergland BE, editor. Handbook of Holocene palaeoecology and palaeohydrology. New York: Wiley; p. 497–505.
van Geel B. 2001. Non-pollen palynomorphs. In: Smol JP, Birks HJB, Last WM, editors. Tracking environmental change using lake sediments, Volume 3: Terrestrial, algal and siliceous indicators. Dordrecht: Kluwer Academic Publishers; p. 99–119.
van Waveren IM. 1992. Morphology of probable planktonic crustacean eggs from the Holocene of the Banda Sea (Indonesia). In: Head MJ, Wrenn JH, editors. Neogene and quaternary dinoflagellate cysts and acritarchs. Dallas (TX): AASP Foundation; p. 89–120.
van Waveren IM. 1994. Tintinnomorphs from the deep-sea sediments of the Banda Sea (Indonesia). Scripta Geologica. 105:27–51.
Vesey-Fitzgerald DF. 1955. Vegetation of the Red Sea coast south of Jedda, Saudi Arabia. The Journal of Ecology. 43(2):477–498.
Wainman CC, Mantle DJ, Hannaford C, McCabe PJ. 2019. Possible freshwater dinoflagellate cysts and colonial algae from the Upper Jurassic strata of the Surat Basin, Australia. Palynology. 43(3):411–422. doi:10.1080/01916122.2018.1451785
Wall D, Warren JS. 1969. Dinoflagellates in Red Sea piston cores. In: Degens ET, Ross DA, editors. Hot brines and recent heavy metal deposits in the Red Sea. Berlin: Springer-Verlag New York Inc., p. 317–328.
Warner BG. 1990. Methods in quaternary ecology#10. Other fossils. Geoscience Canada. 16(4):231–242.